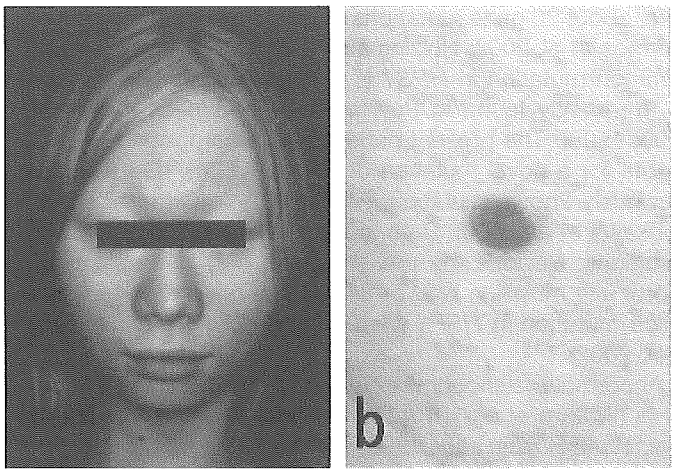

Figure 1
Clinical features of the Hermansky–Pudlak Syndrome 1 patient. (*a*) The face of the patient. The skin is pale and the hair is bright gold in color as a Japanese girl. Her eyes are pale red-brown (not shown). (*b*) A pinkish papule, melanocytic nevus, 5 mm in diameter, was present on her neck.

that IVS5 + 5G > A is a pathologic mutation with an experimental evidence, which results in the exon 5 skipping (Suzuki *et al*, 2004). Then we investigated an aberrant splice pattern caused by the IVS6 + 1G > A mutation with the RT-PCR method using the patient RNA. The allele with the IVS6 + 1G > A mutation was amplified with primers spanning around exons 5–7. This primer set would not amplify the transcript derived from another allele with IVS5 + 5G > A which defected exon 5 because of the exon 5 skipping. The result showed that, in the transcript, next GT site within intron 6 (IVS6 + 44) was used for a splice donor site, resulting in a frameshift in the mutant mRNA (Fig 2*c*).

Histological and ultrastructural findings of a pigmented nevus in HPS Light microscopy of the skin sample from the papule of the patient showed that cuboidal or oval cells with round nuclei were clustered in the dermis (Fig 3*a*). A small number of nevus cells contained melanin pigment (Fig 3*b*). Electron microscopy revealed that melanocytes in the epidermis contained mainly premature melanosomes in the cytoplasm, although a few electron dense, mature melanosomes were seen (Fig 4*a*). Most of the melanosomes were in stage I or II, and stage IV melanosomes were rarely seen.

The nevus cells in the dermis contained abundant vesicles of a similar size to that of normal melanosomes (Fig 4*b*), ceroid-like structures and electron-dense pigment within these vesicles (Fig 4*c*), whereas only a small number of those vesicles were also observed in the epidermal melanocytes (Fig 4*a*). In addition, remarkable, large electron-dense structures, 0.7 μm in diameter were seen at the periphery of the trans-Golgi network (Fig 4*d*). These abnormal structures, included large membranous structures, large

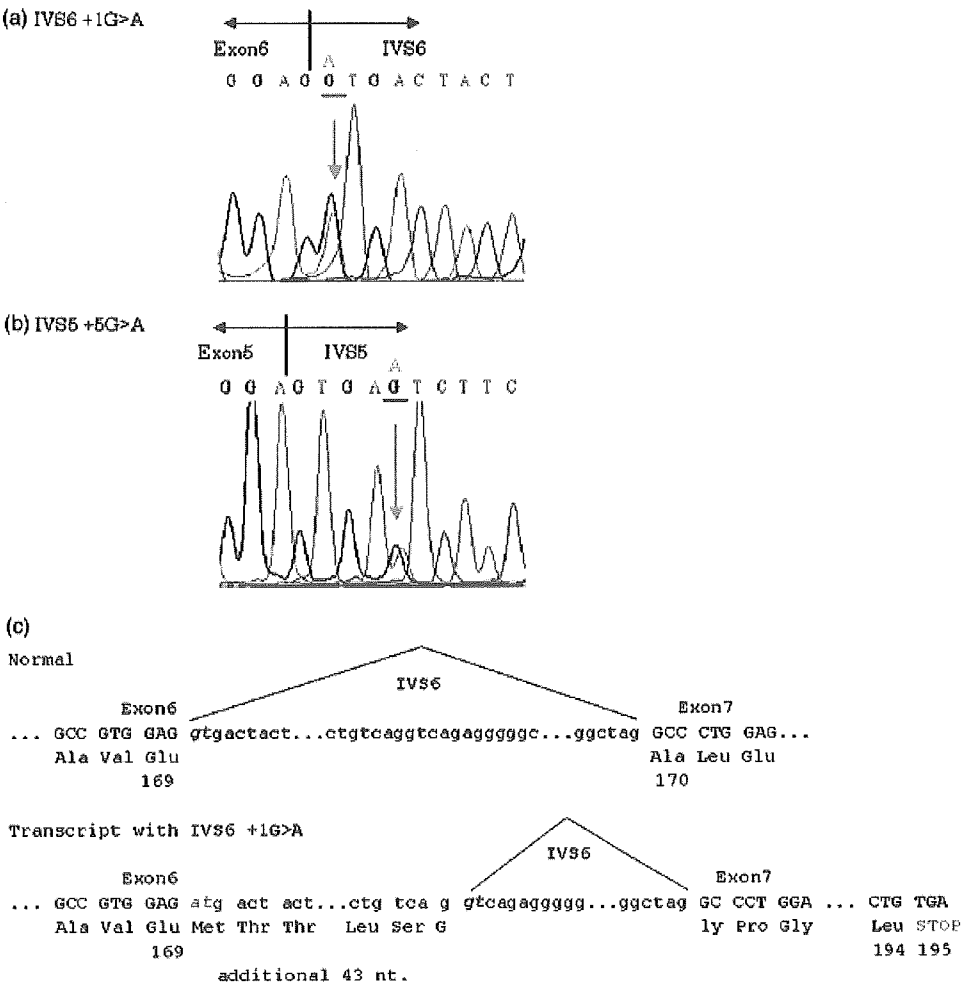

Figure 2
HPS gene mutations and altered splicing in the patient. Direct DNA sequence analysis of the splice donor sites in IVS6 (*a*) and IVS5 (*b*) in the *HPS1* gene. In IVS6, + 1G > A was detected and in IVS5, + 5G > A mutation was identified. (*c*) A mutation of G to A at the first base of IVS6 abolished the 5′ splice site. RT-PCR and DNA sequence analysis showed that the corresponding mRNA was aberrantly spliced, using a cryptic 5′ splice site within IVS6, which resulted in a frameshift.

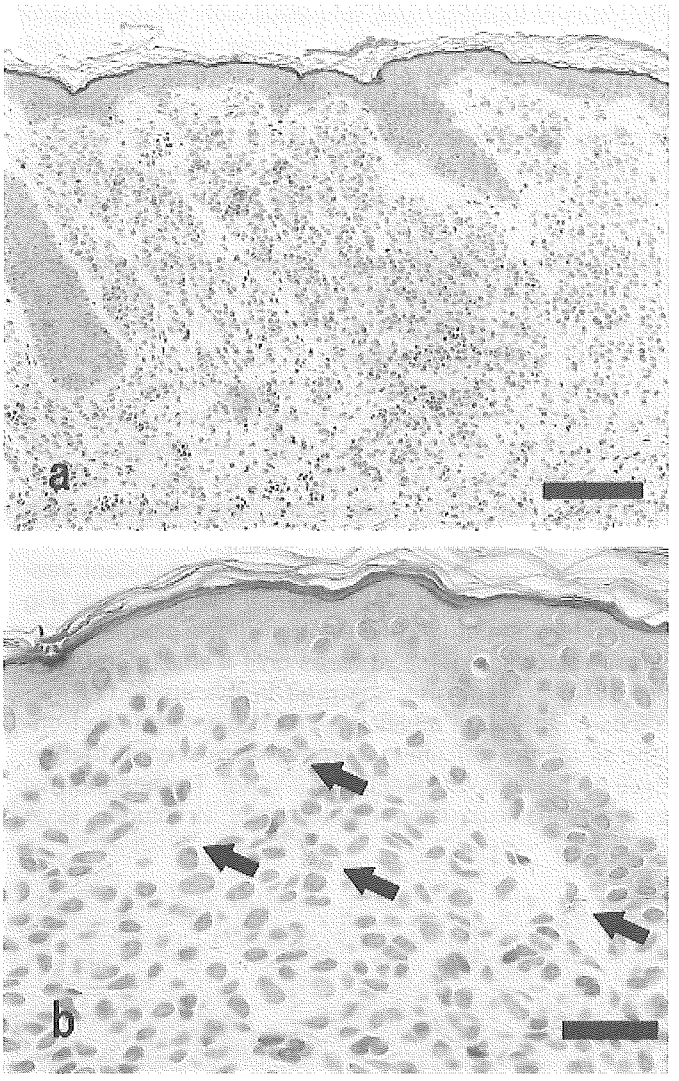

Figure 3
Microscopic features of the pinkish melanocytic nevus on her neck. (*a*) Abundant nevus cells are aggregated in the dermis (hematoxylin and eosin, *scale bar*: 80 μm). (*b*) A few nevus cells contain melanin pigment (*arrows*) (hematoxylin and eosin, *scale bar*: 30 μm).

electron-dense structures, and immature vesicles were remarkably abundant in the nevus cells compared with other cells including epidermal melanocytes.

Electron microscopy showed that, in a control melanocytic nevus of a healthy female, mature melanosomes were scattered and partly aggregated presumably as autophagic vacuoles in the cytoplasm (Fig 4*e*). Neither giant melanosomes nor aberrant vesicles were observed.

Discussion

HPS comprises a group of heterozygous disorders that result from abnormal vesicle formation and protein trafficking. At least, seven human HPS subtypes have been identified (HPS1–7).

HPS1 gene was mapped 10q23 (Fukai *et al*, 1995; Wildenberg *et al*, 1995). It has an open reading frame of 2103 bp, and is divided into 20 exons (Oh *et al*, 1996). To date, about 20 gene mutations in *HPS1* have been reported (Hermos *et al*, 2002; Huizing and Gahl, 2002), and the most common mutation in *HPS1* is a 16 bp duplication in exon 15, frequently found in Puerto Rican pedigrees (Oh *et al*, 1996, 1998). The present patient was a compound heterozygote for a novel mutation of *HPS1*, IVS6+1G>A and a previously known mutation, IVS5+5G>A (Oh *et al*, 1998; Horikawa *et al*, 2000). Both mutations are splice donor site mutations. Besides the present case, only one splice acceptor site mutation IVS17−2A>C has been reported as a splice mutation in *HSP1* (Oetting and King, 1999; Hermos *et al*, 2002).

Abnormal melanosomes have been reported in HPS patients (Witkop *et al*, 1973; Frenk and Lattion, 1982; Boissy *et al*, 1998; Husain *et al*, 1998) and in murine models of HPS (Nguyen and Wei, 2004). HPS1 protein has been thought to function in trafficking molecules to lysosome-related organelles and to be closely related to the formation of lysosome-related organelles. Especially in melanocytes, the HPS1 protein was thought to be involved in sorting melanosome-specific molecules and in formation of early vesicles (premelanosomes) from the trans-Golgi network (Huizing and Gahl, 2002). Previous reports also revealed that melanocytes in HPS patients had exclusively premature melanosomes (Witkop *et al*, 1973; Frenk and Lattion, 1982; Boissy *et al*, 1998; Husain *et al*, 1998). Because of the fact that nevus cells frequently show high melanin producing activity, we hypothesized that melanocytic nevus might show exaggerated abnormalities compared with melanocytes in the epidermis.

Our ultrastructural observation of nevus cells in the HPS patient revealed abnormal vesicles, large membranous structures, and large electron-dense structures, whereas those structures were scarcely seen in epidermal melanocytes of the patient. Many of those abnormal structures retained small amount of pigmentation, elliptical shape, or striations characteristic to melanosomes, and they were thought to be aberrant melanosomes, although we could not excluded the possibility that some of the vesicles were of lysosomal origin. These include abnormal immature melanosomes, large membranous structures, and remarkable large electron-dense structures (giant melanosomes), which were observed abundantly in the periphery to the trans-Golgi network and were thought to be representing trafficking defects, characteristic to HPS. We have utilized genetic analysis and blood clotting assessment for the diagnosis of HPS, and it is true those tests are highly useful. We think ultrastructural analysis of nevus cells can be used as an additional diagnostic procedure.

Giant melanosomes have also been demonstrated in melanocytes from non-Puerto Rican HPS patients (Frenk and Lattion, 1982; Lattion *et al*, 1983; Schallreuter *et al*, 1993; Horikawa *et al*, 2000). Among the patients showing giant melanosomes, mutations were detected only in two patients and both patients had identical mutations, IVS5+5G>A. Those abnormal melanosomes have never been observed in Puerto Rican HPS patients. Horikawa *et al* (2000) speculated that this distinction might be because of the HPS1 gene mutation sites and nature of the defects. Mutation site and/or the nature of IVS5+5G>A lesion might affect vesicle–vesicle fusion, which would result in the

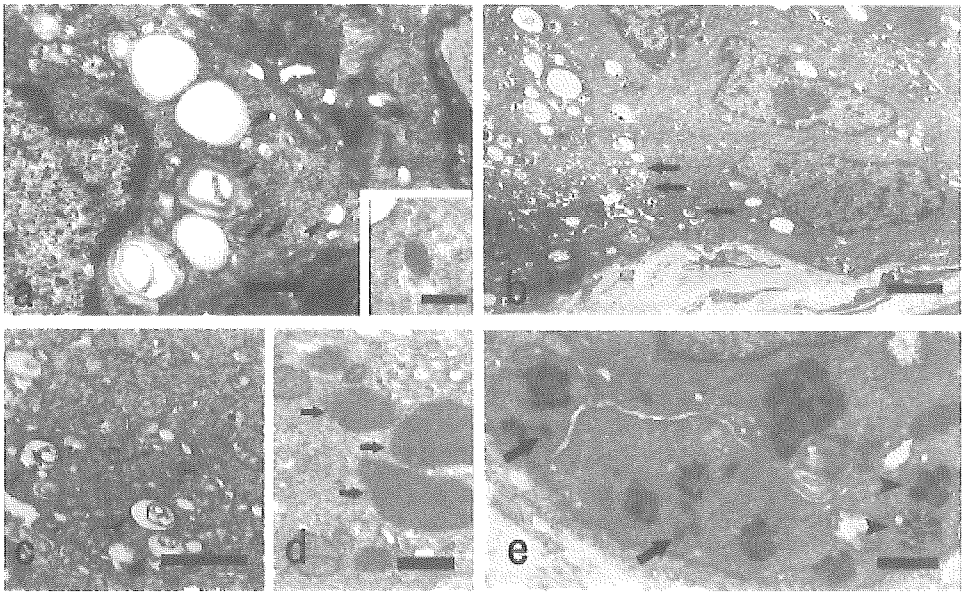

Figure 4
Electron microscopic features of the pinkish melanocytic nevus in Hermansky–Pudlak syndrome 1 patient. (*a*) In the epidermal melanocytes, the majority of melanosomes were in stage I or II (*arrows*) (*scale bar*: 5 μm). A few vesicles (*arrowheads*) were observed. A small number of mature melanosomes were seen (*inset*, *scale bar*: 0.4 μm). (*b*) In the dermal nevus cells, a large number of vacuoles and vesicles (*arrows*) were seen (*scale bar*: 2 μm). (*c*) Vesicles of a similar size to melanosomes (*arrowheads*) were seen and ceroid-like structures and electron-dense pigments were observed in these vesicles (*scale bar*: 1 μm). (*d*) Remarkable large, electron-dense structures (*arrows*), putative giant melanosomes were seen close to the trans-Golgi network (*scale bar*: 0.3 μm). (*e*) In the control nevus cells, abundant mature melanosomes (*arrows*) were observed, and some of those melanosomes were aggregated (*arrowheads*) (*scale bar*: 4 μm). There were no giant melanosomes and abnormal vesicles.

formation of large membranous structures and giant melanosomes as observed in the nevus cells in our HPS patient.

Interestingly, giant melanosomes are also seen in patients with Chediak–Higashi syndrome (CHS), a lysosomal disorder that also presents as oculocutaneous albinism, similar to HPS (Zelickson *et al*, 1967). CHS protein is considered to be a negative regulator of vesicle–vesicle fusion and impaired CHS protein function that promotes formation of large vesicles, such as giant melanosomes (Huizing *et al*, 2001; Marks and Seabra, 2001).

To our knowledge, this is the first report describing ultrastructural features of a nevus cell in an HPS patient. This study revealed that characteristic abnormalities because of protein trafficking defects, aberrant immature melanosomes, large membranous structures, and remarkable large electron-dense structures in the vicinity of the trans-Golgi network, were more clearly demonstrated in the cells in the melanocytic nevus than in other cell types including the epidermal melanocytes. These characteristic ultrastructural findings in nevus cells could provide important clues to further understanding of the pathomechanism of HPS.

Materials and Methods

Mutation detection Using a genomic DNA purification kit (QIAGEN, Valencia, California), genomic DNA was isolated from peripheral blood of the patient. Her *HPS1* gene was amplified from her genomic DNA by PCR using the primers and PCR conditions described previously (Bailin *et al*, 1997). The amplified fragments were then screened for mutations by simultaneous analyses of single-stranded conformation polymorphisms and heteroduplexes method (Spritz *et al*, 1992). PCR products showing aberrant patterns were reamplified and sequenced directly. For RT-PCR analysis RNA was extracted from mononuclear cells in the peripheral blood. The primers for RT-PCR were EX5cf; 5′-TGTGGACGGTCATCTTATCC-3′ in exon 5 and EX7cr; 5′-GGTGTTGACAGCCTGGATGA-3′ in exon 7.

Ultrastructural observations A papule on the patient's neck was resected for morphological observation. In addition, a skin sample of a control melanocytic nevus was obtained from a 29-y-old unrelated female. The pigmented lesion had been present on her back for 10 y. Skin biopsy samples were fixed in 2% glutaraldehyde solution, post-fixed in 1% OsO_4, dehydrated, and embedded in Epon 812 (Perry *et al*, 1987). The samples were sectioned at 1 μm thickness for light microscopy and thin sectioned for electron microscopy (70 nm thick). The histological sections were stained by the method of Richardson *et al* (1960). The thin sections were stained with uranyl acetate and lead citrate (Reynolds, 1963) and examined in a transmission electron microscope.

The medical ethical committee of Hokkaido University approved all described studies. The study was conducted according to Declaration of Helsinki Principles. Participants gave their written informed consent.

DOI: 10.1111/j.0022-202X.2005.23743.x

Manuscript received August 5, 2004; revised January 19, 2005; accepted for publication January 24, 2005

Address correspondence to: Ken Natsuga, MD, Department of Dermatology, Hokkaido University Graduate School of Medicine, North 15 West 7, Kita-ku, Sapporo 060-8638, Japan. Email: natsuga@med.hokudai.ac.jp

References

Anikster Y, Huizing M, White J, *et al*: Mutation of a new gene causes a unique form of Hermansky–Pudlak syndrome in a genetic isolate of central Puerto Rico. Nat Genet 28:376–380, 2001

Bailin T, Oh J, Feng GH, Fukai K, Spritz RA: Organization and nucleotide sequence of the human Hermansky–Pudlak syndrome (HPS) gene. J Invest Dermatol 108:923–927, 1997

Boissy RE, Zhao Y, Gahl WA: Altered protein localization in melanocytes from Hermansky–Pudlak syndrome: Support for the role of the HPS gene product in intracellular trafficking. Lab Invest 78:1037–1048, 1998

Dell'Angelica EC, Shotelersuk V, Aguilar RC, *et al*: Altered trafficking of lysosomal proteins in Hermansky–Pudlak syndrome due to mutations in the 3A subunit of the AP-3 adaptor. Mol Cell 3:11–21, 1999

Frenk E, Lattion F: The melanin pigmentary disorder in a family with Hermansky–Pudlak syndrome. J Invest Dermatol 78:141–143, 1982

Fukai K, Oh J, Frenk E, Almodovar C, Spritz RA: Linkage disequilibrium mapping of the gene for Hermansky–Pudlak syndrome to chromosome 10q23.1–q23.3. Hum Mol Genet 4:1665–1669, 1995

Hermansky F, Pudlak P: Albinism associated with hemorrhagic diathesis and unusual pigmented reticular cells in the bone marrow: Report of two cases with histochemical studies. Blood 14:162–169, 1959

Hermos CR, Huizing M, Kaiser-Kupfer MI, Gahl WA: Hermansky–Pudlak syndrome type 1: Gene organization, novel mutations, and clinical-molecular review of non-Puerto Rican cases. Hum Mutat 20:482, 2002

Horikawa T, Araki K, Fukai K, Ueda M, Ueda T, Ito S, Ichihashi M: Heterozygous *HPS1* mutations in a case of Hermansky–Pudlak syndrome with giant melanosomes. Br J Dermatol 143:635–640, 2000

Huizing M, Anikster Y, Gahl WA: Hermansky–Pudlak syndrome and Chediak–Higashi syndrome: Disorders of vesicle formation and trafficking. Thromb Haemost 86:233–245, 2001

Huizing M, Gahl WA: Disorders of vesicles of lysosomal lineage: The Hermansky–Pudlak syndromes. Curr Mol Med 2:451–467, 2002

Husain S, Marsh E, Saenz-Santamaria MC, McNutt NS: Hermansky–Pudlak syndrome: Report of a case with histological, immunohistochemical and ultrastructural findings. J Cutan Pathol 25:380–385, 1998

Lattion F, Schneider P, Da Prada M, Lorez HP, Richards JG, Picotti GB, Frenck E: Hermansky–Pudlak syndrome in a Valais village. Helv Paediatr Acta 38:495–512, 1983

Li W, Zhang Q, Oiso N, *et al*: Hermansky–Pudlak syndrome type 7 (HPS-7) results from mutant dysbindin, a member of the biogenesis of lysosome-related organelles complex 1 (BLOC-1). Nat Genet 35:84–89, 2003

Marks MS, Seabra MC: The melanosome: Membrane dynamics in black and white. Nat Mol Rev Cell Biol 2:738–748, 2001

Nguyen T, Wei ML: Characterization of melanosomes in murine Hermansky–Pudlak syndrome: Mechanisms of hypopigmentation. J Invest Dermatol 122:452–460, 2004

Oetting WS, King RA: Molecular basis of albinism: Mutations and polymorphisms of pigmentation genes associated with albinism. Hum Mutat 13:99–115, 1999

Oh J, Bailin T, Fukai K, *et al*: Positional cloning of a gene for Hermansky–Pudlak syndrome, a disorder of cytoplasmic organelles. Nat Genet 14:300–306, 1996

Oh J, Ho L, Ala-Mello S, *et al*: Mutation analysis of patients with Hermansky–Pudlak Syndrome: A frameshift hot spot in the HPS gene and apparent locus heterogeneity. Am J Hum Genet 62:593–598, 1998

Perry TB, Holbrook KA, Hoff MS, Hamilton EF, Senikas V, Fisher C: Prenatal diagnosis of congenital nonbullous ichthyosiform erythroderma (lamellar ichthyosis). Prenat Diag 7:145–155, 1987

Reynolds ES: The use of lead citrate at high pH as an electron-opaque stain in electron microscopy. J Cell Biol 17:208–212, 1963

Richardson KC, Jarett L, Finke EH: Embedding in epoxy resins for ultrathin sectioning in electron microscopy. Stain Technol 35:313–323, 1960

Schallreuter KU, Frenk E, Wolfe LS, Witkop CJ, Wood JM: Hermansky–Pudlak syndrome in a Swiss population. Dermatol 187:248–256, 1993

Spritz RA, Holmes SA, Ramesar R, Greenberg J, Curtis D, Beighton P: Mutations of the KIT (mast/stem cell growth factor receptor) proto-oncogene account for a continuous range of phenotypes in human piebaldism. Am J Hum Genet 51:1058–1065, 1992

Suzuki T, Ito S, Inagaki K, Suzuki N, Tomita Y, Yoshino M, Hashimoto T: Investigation on the IVS5 + 5G → A splice site mutation of *HPS1* gene found in Japanese patients with Hermansky–Pudlak syndrome. J Dermatol Sci 36:106–8, 2004

Suzuki T, Li W, Zhang Q, *et al*: Hermansky–Pudlak syndrome is caused by mutations in HPS4, the human homolog of the mouse light-ear gene. Nat Genet 30:321–324, 2002

Wildenberg SC, Oetting WS, Almodovar C, Krumwiede M, White JG, King RA: A gene causing Hermansky–Pudlak syndrome in a Puerto Rican population maps to chromosome 10q2. Am J Hum Genet 57:755–765, 1995

Witkop CJ Jr, Hill CW, Desnick S, *et al*: Ophthalmologic, biochemical, platelet, and ultrastructural defects in the various types of oculocutaneous albinism. J Invest Dermatol 60:443–456, 1973

Zelickson AS, Windhorst DB, White JG, Good RA: The Chediak–Higashi syndrome: Formation of giant melanosomes and the basis of hypopigmentation. J Invest Dermatol 49:575–580, 1967

Zhang Q, Zhao B, Li W, *et al*: Ru2 and Ru encode mouse orthologs of the genes mutated in human Hermansky–Pudlak syndrome types 5 and 6. Nat Genet 33:145–153, 2003

THE JOURNAL OF GENE MEDICINE
J Gene Med 2005; 7: 664–671.
Published online 17 January 2005 in Wiley InterScience (www.interscience.wiley.com). **DOI:** 10.1002/jgm.709

RESEARCH ARTICLE

Direct injection of plasmid DNA into the skin induces dermatitis by activation of monocytes through toll-like receptor 9

D. Sawamura[1]*
R. Abe[1]
M. Goto[1]
M. Akiyama[1]
H. Hemmi[2]
S. Akira[2]
H. Shimizu[1]

[1]*Department of Dermatology, Hokkaido University Graduate School of Medicine, Sapporo, Japan*

[2]*Department of Host Defense, Research Institute for Microbial Diseases, Osaka University and ERATO, Japan Science and Technology Corporation, Japan*

*Correspondence to: D. Sawamura, Department of Dermatology, Hokkaido University Graduate School of Medicine, N15 W7, Sapporo, 060-8638, Japan. E-mail: smartdai@med.hokudai.ac.jp

Received: 3 July 2004
Revised: 25 September 2004
Accepted: 27 September 2004

Abstract

Background Direct injection of naked DNA into skin can be efficiently used to transfer genes into keratinocytes *in vivo*. However, bacterial DNA is known to be a potent stimulus for vertebrate immune cells and immune systems. Towards the clinical use of this method, this study examined whether the application of plasmid DNA by direct injection induces any adverse skin effects.

Methods Several plasmid preparations were prepared and directly injected into rat and human skin. Migration, IL-6 production, and reactive oxygen production assays were performed to determine the type of the primary cells responsible for the reaction. Involvement of toll-like receptor (TLR) 9 was examined by experiments using TLR9-knockout mice.

Results Injection of several plasmid preparations into rat and human skin resulted in an inflammatory reaction at the treated site. Contamination by endotoxin in the plasmid preparation was shown to worsen this skin inflammation reaction. Immunohistochemical analysis showed that the infiltrating cells in the skin lesions were predominantly monocytes and neutrophils. Further experiments examining migration, IL-6 production, and reactive oxygen production indicated that the primary responsible cells were monocytes rather than neutrophils. Since it was recently shown that cytosine-guanosine dinucleotide (CpG) motif is critical for immune reaction induction in bacterial DNA and cellular responses were mediated by TLR9, we injected plasmids into the ear skin of TLR9-knockout mice. A decrease in ear swelling was noted in the knockout mice, compared to controls, suggesting that plasmid-DNA-induced dermatitis was mediated mostly by TLR9.

Conclusions This study demonstrates that injection of plasmid DNA induces skin inflammation initiated by monocyte activation via TRL9. We should therefore attempt to counteract this dermatitis during the clinical use of the naked DNA injection method in skin. Copyright © 2005 John Wiley & Sons, Ltd.

Keywords gene therapy; keratinocyte; naked DNA

Introduction

Gene therapy is a promising technique to treat patients with intractable diseases and is now approved worldwide [1]. One of main target cells in gene therapy for skin diseases is the epidermal keratinocyte. Keratinocyte gene

therapy is primarily directed toward skin diseases with a single gene deficiency, but is also applicable to skin cancers and intractable inflammatory skin diseases [2,3]. Keratinocyte gene therapy can also be extended to systemic diseases in an attempt to deliver gene products into the general circulation [2,4]. Successful keratinocyte gene therapy requires the development of highly efficient methods of gene transfer into keratinocytes. Several methods including viral- [5] and non-viral- [6] mediated transduction have been reported during *in vivo* gene transfer.

Among those methods, a simple, safe and relatively efficient method is the direct injection of naked DNA [7], in which intradermally injected plasmid DNA is taken up and expressed by keratinocytes *in vivo*. This method can directly introduce the gene even into human keratinocytes [8,9] and can initiate biological effects from the gene product within the human skin [10]. Although this method is thought to involve a complex process, the detailed mechanisms of uptake of DNA by keratinocytes have not yet been fully elucidated.

The naked DNA injection method can also be used to transfer genes into myocytes. Intramuscular injection of plasmid DNA expressing cytokine genes into patients with critical limb ischemia has provided favorable results by increasing the rate of angiogenesis [11,12]. Thus, gene transfer into keratinocytes using the naked DNA method also harbors great potential for treating intractable skin diseases. However, plasmid DNA may induce different types of reactions since the skin has more immunological functions than muscle. Towards the clinical use of this method for gene transduction in keratinocyte gene therapy, we have examined whether the injection of naked plasmid DNA could induce any adverse dermatological effects.

Materials and methods

Preparation of plasmid DNA

Plasmid Bluescript II KS(+) (Stratagene, La Jolla, CA, USA: GenBank accession no. X52327) was used for these experiments. The Bluescript II (BS) is a cloning vector designed to simplify commonly used cloning and sequencing procedures, and is used worldwide.

We obtained plasmid DNA (Ordinary BS) utilizing ordinary preparation techniques with cultured bacteria using a Qiagen plasmid kit (Qiagen, Germany). Endofree BS was also prepared using an Endofree plasmid kit (Qiagen), in which bacterial lysates are cleared by filtration with QIA filter cartridges and plasmid DNA is purified by gravity-flow Qiagen anion-exchange tips. The instructions mention that plasmid DNA purified with this kit contains only negligible amounts of endotoxin. To further reduce the endotoxin contamination, we utilized endotoxin-removing gel, Detox-Gel (Pierce, Rockford, IL, USA), in which polymixin B immobilized in agarose gel inactivates endotoxin. We obtained Gel-treated BS by treating Endofree BS with column chromatography containing the removing gel. Calf thymus DNA (Calf DNA; Sigma, St. Louis, IL, USA) was used as the control mammalian DNA. Endotoxin contamination was assayed by the Limulus test (WAKO, Osaka, Japan) and the values represent the mean ± SD of the five samples.

Injection of plasmid DNA into the skin

To evaluate the effects of plasmid DNA in the skin, we injected DNA into Hirosaki hairless rats and control human individuals. The DNA samples were diluted in saline to obtain plasmid DNA at an appropriate concentration and were then intradermally injected into the rat and human skin using a 29 G needle. We injected saline only as control. Since we needed to inject plasmid DNA as superficially as possible into the dermis for the proper transfer of DNA into rat keratinocytes [13], we also tried to inject superficially in this study. The injected volume was 30 μl per injection site. The injected site was observed carefully 48 h after the injection and the skin condition was graded according to the following scores, 0: no reaction, 1: slight erythema, 2: erythema, 3: indurated erythema, 4: erythema with a hemorrhage or blister. We used six rats for each experiment and three series of dilution were injected into the back skin of each rat. Also three normal human volunteers were enrolled for each experiment and three series of dilution were injected into bilateral flexor aspects of forearms. The inflammatory index was calculated as the mean of scores of three areas. The values shown in this study represent the mean ± SD of six individual indices. Experiments were repeated three times. Skin biopsy specimens were taken from the treated sites several times after introduction. This study was approved by the Ethical Committee at Hokkaido University Graduate School of Medicine. Informed consent was obtained from all participating individuals.

Migration assay

Human monocytes and neutrophils were obtained from venous blood from normal volunteers by a routine method. Briefly, erythrocytes were sedimented by addition of 6% dextran saline solution, and then the neutrophil and mononuclear cell fractions were obtained by centrifugation with Lymphoprep (Nycomed Pharma, Oslo, Norway). The mononuclear cells were further allowed to adhere to sterile tissue culture plates for 30 min and were then treated with 1 mM EDTA-PBS containing 5% serum. Monocyte or neutrophil migration was performed using 24-well transwell plates with a 5-nm pore size, untreated (monocyte) or endothelialized (neutrophil) polycarbonate membrane. Plasmid DNA or Calf DNA (25 μg/ml) was placed in the upper, lower or both upper and lower chambers, and then 1×10^5 monocytes, or 1×10^6 neutrophils, were seeded in the

upper chamber. Neither plasmid DNA nor calf thymus DNA was added in control. After incubation for 3 h (monocytes) or 1.5 h (neutrophils), migrated cells were counted.

Monocyte IL-6 production

Human monocytes were prepared by the methods mentioned above. The cells were prepared at a concentration of 2.0×10^5/ml and were cultured in 24-well plates in the presence or the absence of plasmid DNA for 24 h. The supernatants were harvested, filtered (using 0.2-μm filters) and stored at −80 °C. By comparing the OD of the samples with a standard curve, the concentration of the IL-6 in the culture supernatant was determined. The ELISA kit (R&D Systems, Minneapolis, MN, USA) was used according to the manufacturer's instruction.

Neutrophil reactive oxygen production

Human neutrophils were prepared by the same method as mentioned above. Production of O_2^- was measured by the rate of reduction of ferricytochrome *c* [14]. Approximately 2.0×10^5 cells were incubated at 37 °C in Tyrode's buffer (2.6 mM KCl, 1 mM $MgCl_2$, 137 mM NaCl, 6 mM $CaCl_2$, 0.1% glucose, and 1 mM Tris, pH 7.4) containing 80 μM cytochrome *c* with or without plasmid DNA. The absorbance of each supernatant was measured in a spectrophotometer at 550 nm. The extinction coefficient of ferricytochrome *c* at 550 nm was taken as 2.1×10^4 M^{-1} cm^{-1}. O_2^- production was expressed as a nanomolar concentration of cytochrome *c* reduced per cell.

Inflammatory reaction in TLR9-knockout mice

The inflammatory reaction induced by plasmid DNA was examined using TLR9-knockout gene mice [15]. We injected 10 μl of plasmid solution into the dorsal and ventral aspects of the right ears of the knockout mice (TLR9 −/−) and wild-type littermates (TLR9 +/+) whereas the left ears were treated with saline. We used seven mice for each experiment. The ear thickness of the mice was then measured using an engineer's micrometer 48 h after the initial injection. The inflammatory reaction was then evaluated by measuring the difference in thickness between the right and left ears. The values represent the mean ± SD of differences in ear thickness of seven individual animals. Experiments were repeated three times.

Statistical analysis of data

Significant differences between groups were evaluated using Student's *t* test.

Results

Plasmid DNA induces an inflammatory reaction in rat skin

First, we prepared Ordinary BS and Endofree BS, subsequently injected various doses of the samples into rat skin intradermally, and observed the treated sites 48 h after the initial treatment. The introduction of the genes into rat keratinocytes using this method usually involved the injection of 3–6 μg plasmid DNA into the site [13]. A dose of 10 μg caused slight erythema using the Ordinary BS sample while the sites of the Endofree BS and Calf DNA samples failed to show any inflammatory reactions (Figure 1A). The inflammatory index (see Materials and methods) using 10 μg of Ordinary BS was 0.75. However, the inflammatory reaction using the Ordinary BS sites increased with the DNA dose. Furthermore, an increase in the dose induced a greater erythematous reaction when using the Endofree BS plasmid (Figure 1A). We did not observe any reaction in the injection sites when Calf DNA (mammalian DNA control) or saline (DNA free vehicle control) was used (data not shown).

Next, we observed over a time course the histological changes in the site of the inflammatory reaction induced by plasmid DNA. Endofree BS (30 μg) was injected into rat skin and the injected site was histologically examined at various time points after injection. We found infiltration of leukocytes in the upper dermis 24 h after gene transfer (Figure 2). The 48 h sample demonstrated significant leukocyte infiltration, telangiectasia and intracellular edema of the epidermis. Afterwards the inflammation gradually decreased.

Presence of endotoxin contamination in plasmid samples

Since we found erythematous reactions even in the Endofree sample, we examined the concentration of endotoxin in the plasmid samples. A high level of endotoxin contamination was observed in the Ordinary BS, while the Endofree BS samples showed only a small amount of endotoxin (Table 1). There was no detectable endotoxin in the Calf DNA and the Gel-treated BS samples. These samples were obtained by passing the Endofree BS samples through a chromatography column to remove the endotoxin contaminants.

Table 1. Contamination of endotoxin in plasmid preparations

Plasmid DNA	Amount of Endotoxin ± SD (EU/μg plasmid DNA)
Ordinay BS	8.5 U/μg ± 1.2
Endofree BS	0.1 U/μg ± 0.02
Gel-treated BS	<0.001 U/μg
Calf thymus DNA	<0.001 U/μg
Saline	<0.001 U/μg

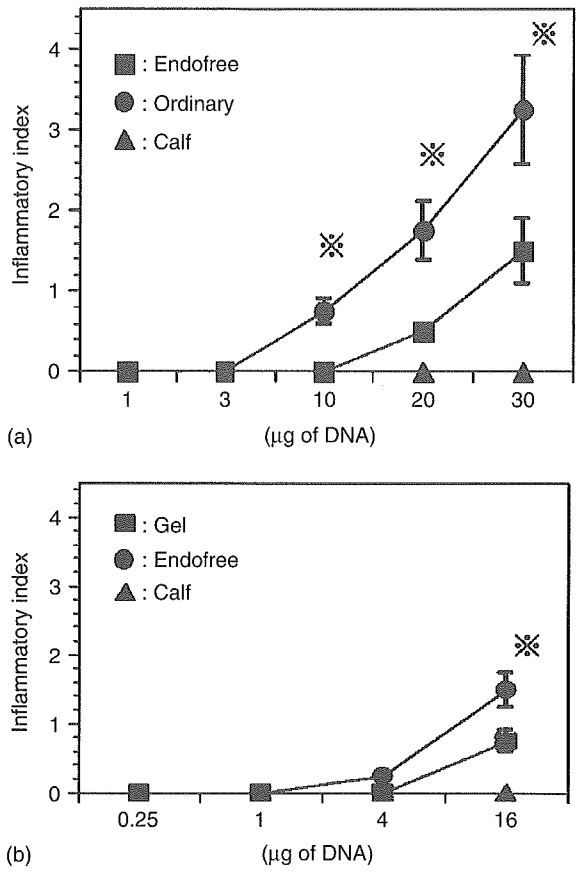

Figure 1. Plasmid DNA induces an inflammatory reaction in rat and human skin. (A) We prepared the Ordinary BS and Endofree BS plasmid DNA. Various doses of the samples were injected into rat skin and the injected site was carefully observed 48 h after the first injection. The values of the inflammatory index shown represents the mean ± SD of six individual indices. At a dose of 10 μg, slight erythema was observed in the Ordinary BS sample. An increased dose induced an erythematous reaction in the Endofree BS plasmid site. No reaction was observed in the Calf DNA injection site (a control for mammalian DNA). Significant differences between the Ordinary and Endofree BS groups in 10, 20 and 30 μg, $^{※}p < 0.01$. (B) We prepared plasmid DNA using the Endofree BS and Gel-treated BS systems. Various doses of the samples were injected into human skin and the injected site was carefully observed 48 h after the injection. The inflammatory index values shown represent the mean ± SD of six individual indexes. At a maximum dose of 16 μg, erythema was observed at sites prepared using the Endofree and Gel-treated BS, and the inflammation of the Endofree was much stronger than that of the Gel-treated BS. No reaction was observed in the Calf DNA treated site representing control mammalian DNA. Significant differences between the Endofree and Gel-treated BS groups in 16 μg, $^{※}p < 0.01$

Plasmid DNA induces an inflammatory reaction in the human skin

Since a high level of endotoxin contamination was observed in the Ordinary BS, we used only the Endofree BS and the Gel-treated BS for the following human experiments. Various doses of the plasmid samples were injected into the flexor aspects of forearms of three volunteers. At a maximum dose of 16 μg, erythema was observed at the sites of the Endofree and Gel-treated BS, and inflammation at the site of the Endofree treatment was considerably stronger that that of the Gel-treated BS site (Figure 1B). The erythematous reaction of both samples became weaker with decreasing DNA concentrations. The sites of Calf DNA and saline did not show any reaction. Histological examination of the 16 μg Endofree section demonstrated dermal infiltration of neutrophils and mononuclear cells (Figure 3). The majority of the infiltrating mononuclear cells were CD3(−), CD4(−) and CD8(−), while expression of CD68 was found, indicating that these cells were monocytes (Figure 3). Histological findings of the 16 μg Gel-treated BS sections were basically the same as that of the Endofree BS sections, but the extent of infiltration at the Endofree injection sites was much greater that that of the Gel-treated BS.

Activation of monocytes by plasmid samples

Since we had identified the infiltrating cells as predominantly monocytes and neutrophils, we then examined which subsets of cells responded primarily to the plasmid DNA samples. Our *in vivo* experiments had suggested that any contamination of endotoxin in the Endofree BS sample could enhance plasmid-DNA-induced inflammation. We used the Gel-treated BS samples in the next experiment, a cell migration assay. Plasmid DNA was added to the upper, lower, or both upper and lower chambers. Migration assays using monocytes showed that the cell numbers of the samples with plasmid in the upper and upper/lower chambers increased whereas that in the lower chamber was constant (Figure 4). Calf DNA had no effect on the cell number when compared with control samples. These results indicated that plasmid DNA enhanced monocyte chemokinesis rather than chemotaxis. However, neutrophil migration assays showed no changes in the cell numbers. Collectively, plasmid DNA directly activates or modulates only monocyte chemokinesis, and not transendothelial neutrophil migration *in vitro*.

To further confirm the extent of monocyte involvement in the inflammatory reactions, we examined what effects the Gel-treated BS has on monocyte IL-6 production and reactive oxygen production by neutrophils. The results suggested that the plasmid DNA increased IL-6 production, while reactive oxygen production was not affected by plasmid DNA (Figure 5). These results also suggested that the primary cells that responded to the plasmid DNA were monocytes rather than neutrophils.

Involvement of TLR9

It was recently shown that cellular responses to the cytosine-guanosine dinucleotide (CpG) motif in bacterial DNA were mediated by TLR9. We therefore examined

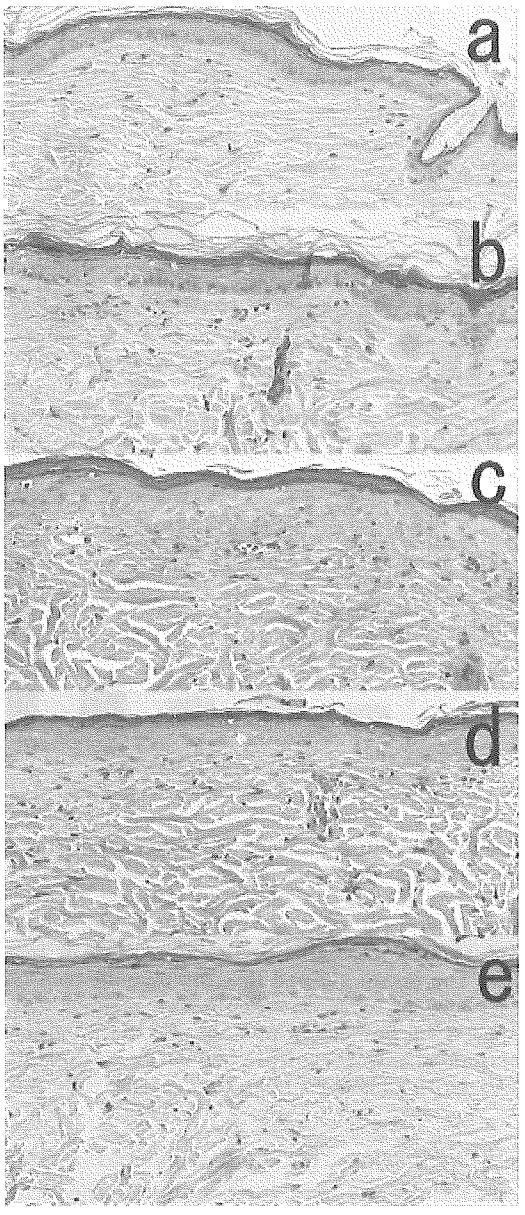

Figure 2. Time course showing the histological changes in the inflammatory reaction induced by plasmid DNA. Endofree BS plasmid DNA (30 μg) was injected into rat skin and the injected site was examined histologically (a) before, and 24 h (b), 48 h (c), 72 h (d), and 96 h (e) after the injection. The 48 h sample demonstrated strong leukocyte infiltration, telangiectasia and intracellular edema of the epidermis

whether there was any involvement of the TRL9 in plasmid-DNA-induced skin inflammation using a TLR9-knockout mouse. We intradermally injected Gel-treated BS plasmid samples and Calf DNA into the ear of TLR9-knockout mice and measured the thickness of the treated ear. An approximate 40% decrease in the ear swelling was noted in the TLR9-deficient (−/−) mice in the plasmid sample as compared with the TRL9 (+/+) littermates (Figure 6). Histological examination of the treated ears also showed similar results (Figure 7). Although prominent leukocyte infiltration and skin thickening was observed in littermates treated with plasmid, this inflammation was clearly inhibited in TLR9

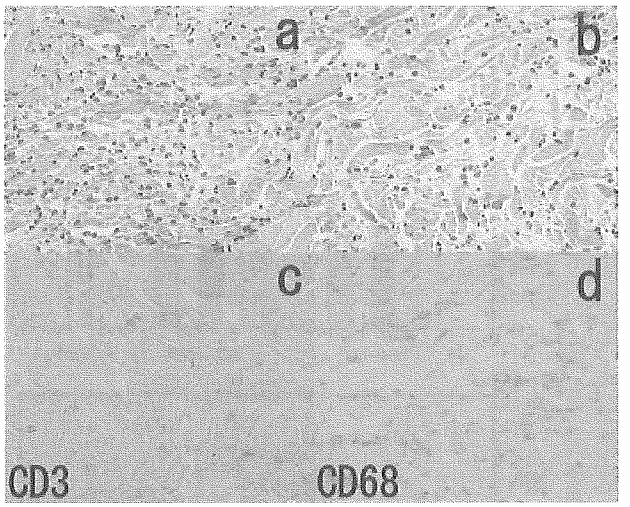

Figure 3. Plasmid-DNA-induced reaction in human skin. (a, b) Histological examination of the 16 μg Endofree (a) and Gel-treated (b) BS-injected sites demonstrated a dermal infiltration of neutrophils and mononuclear cells. (c, d) The majority of the infiltrating mononuclear cells were CD3(−) (c) while there was expression of CD68(+) cells (d)

(−/−) mice. This result suggested that plasmid-DNA-induced dermatitis was also mediated by TLR9 expressed by monocytes.

Discussion

Intradermally injected plasmid DNA is taken up and expressed by keratinocytes *in vivo*. This technique alone or combined with the other methods is a promising candidate clinical treatment for keratinocyte gene therapy. In fact, the injection of plasmid DNA encoding vascular endothelial growth factor into the skeletal muscle has been successful in patients with critical limb ischemia, resulting in clinical improvement [11]. However, bacterial DNA including many plasmids also induces a strong inflammatory reaction in the respiratory tract and knee joint when applied to these areas [16,17]. Therefore, in this study we examined whether bacterial plasmid DNA introduced into the skin would induce any adverse cutaneous effects.

One of the problems in the use of bacterial DNA is endotoxin contamination, which produces an apparent dermatitis [18]. Thus, attempts should be made to decrease the levels of endotoxin contamination in plasmid DNA preparations. In clinical trials using intramuscular injection, the vascular endothelial growth factor gene plasmids were obtained using a Qiagen preparation kit [11]. In this study, we first injected the Ordinary and Endofree BS into normal rat skin. Both samples elicited cutaneous inflammation, although the inflammatory reaction in the Ordinary BS treatment was stronger than that of Endofree BS sites. We hypothesized that the endotoxin remaining in plasmid samples was likely to be at least partially responsible for the dermatitis and

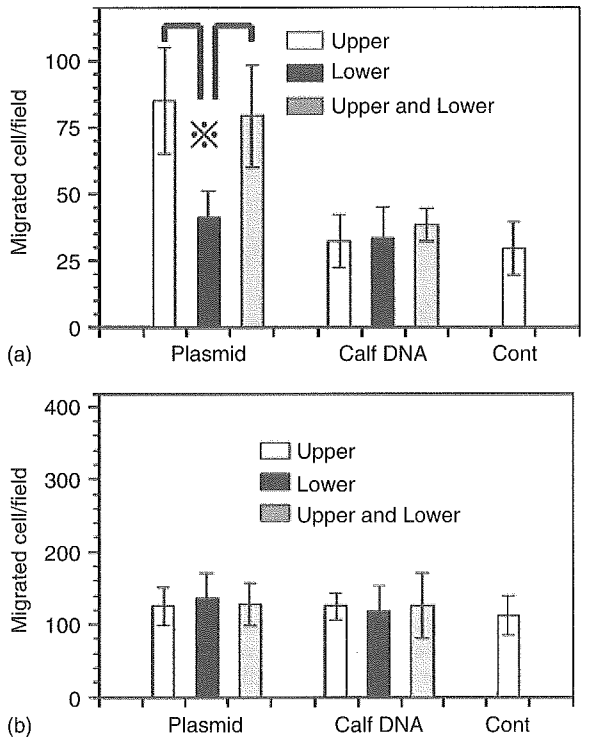

Figure 4. Plasmid DNA activates only monocyte chemokinesis, not transendothelial neutrophil migration. Human monocytes and neutrophils, obtained from venous blood from normal control volunteers, were subjected to migration assays using the Gel-treated BS. The values were expressed as the mean ± SD of between four to six samples. (A) The migration assays showed that the cell numbers of the samples with plasmid in the upper and upper/lower chambers increased whereas that in the lower camber was constant. The Calf DNA did not show any effect on the cell number. Control: no DNA samples. Significant differences between the upper and lower, and between the lower and upper/lower groups, $^{※}p < 0.01$. (B) The neutrophil migration assay failed to show any change the number of cells

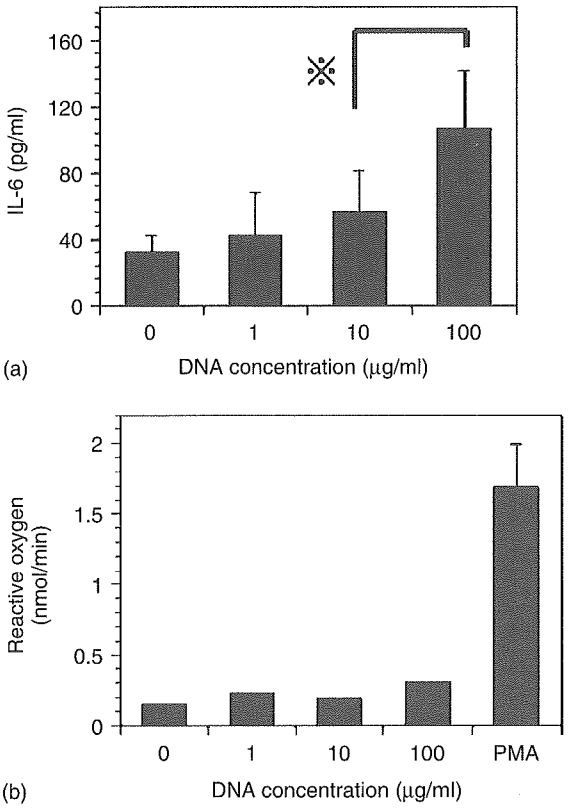

Figure 5. Plasmid DNA increases IL-6 production, but does not affect reactive oxygen production. We incubated monocytes and neutrophils with the gel-treated BS, and then measured IL-6 production and reactive oxygen production, respectively. The values were expressed as the mean ± SD of four to six samples. The results showed that the plasmid DNA increased IL-6 production in a dose-dependent manner (A), while reactive oxygen production was not affected by plasmid DNA concentration (B). PMA: positive control. Significant differences between the 10 μg/ml and 100 μg/ml groups, $^{※}p < 0.02$

we therefore measured the endotoxin content in these samples. The results showed that a high and low level of endotoxin was detected in both the Ordinary and Endofree samples, respectively. There was no detectable endotoxin in the Calf DNA and the Gel-treated BS. Previous reports have applied plasmid DNA at 50 μg in 100 μl solution (0.5 μg/μl) but have failed to describe any skin changes after delivery [19,20]. This study also found that Endofree BS plasmids induced an erythematous reaction not at 10 μg in 30 μl solution (0.33 μg/μl), but at 20 μg in 30 μl solution (0.67 μg/μl).

In human skin, a maximum dose of 16 μg plasmid DNA induced an erythematous reaction at sites of both the Endofree BS and Gel-treated BS samples. Inflammation at the sites of the Endofree samples was much greater than that of the Gel-treated BS (Figure 1). The reaction at injection sites of Calf DNA and saline failed to show any inflammation. The results indicated that plasmid DNA itself could cause an inflammatory skin reaction while endotoxin remaining in the Endofree BS samples only marginally worsened the reaction. Histological examination of these inflammation sites showed infiltrations of neutrophils and mononuclear cells in the dermis, and further immunohistochemistry demonstrated that the infiltrating mononuclear cells were predominantly CD3(−), CD4(−), CD8(−), CD68(+) compatible with monocytes (Figure 3).

To further determine which immune cells played a major role in this plasmid-DNA-induced dermatitis, we performed several experiments including migration, IL-6 production, and reactive oxygen species production assays. The results indicated that the primary responsible cells were monocytes rather than neutrophils. A previous study has shown that arthritis can be induced by bacterial DNA and that this is also mediated by monocytes [17]. This suggests that innate immunity related to monocytes might be involved in plasmid-induced dermatitis rather than the acquired immunity related with lymphocytes.

As mentioned above, bacterial DNA is a potent stimulus for vertebrate immune cells and systems. Specifically, the presence of unmethylated cytosine-guanosine dinucleotide (CpG) sequence motifs is responsible for its immunostimulatory activity [21,22]. CpG motifs are present more frequently in bacterial DNA than vertebrate DNA, and the cytosines in CpG dinucleotide sequences

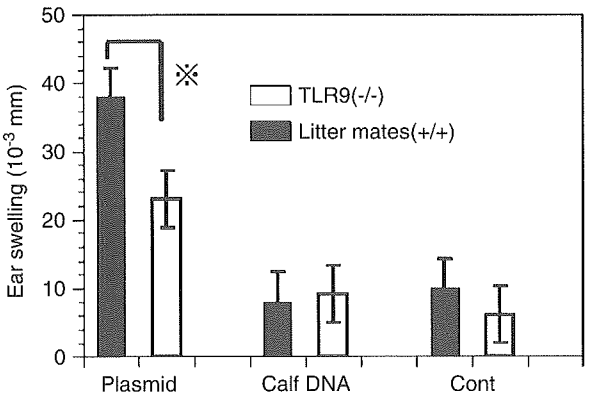

Figure 6. Involvement of TLR9 in the plasmid-DNA-induced reaction. We injected the Gel-treated BS and Calf DNA into the right ears of TLR9-knockout mice (TLR9 −/−) and wild-type littermates (TLR9 +/+) whereas the left ears were injected with saline alone. The ear thickness of each mouse was measured 48 h after the first injection. The inflammatory reaction was then evaluated by measuring the difference in thickness between the right and left ears. The values represent the mean ± SD of seven individual differences. A significant decrease in the ear swelling in TLR9 (−/−) mice was observed in plasmid samples as compared with TRL9 (+/+) mice. $^{※}p < 0.01$

in vertebrate DNA are highly methylated in contrast to bacterial DNA. Recent findings indicate that the toll-like receptor (TLR) 9 is critical in the recognition of CpG motifs of bacterial DNA [15]. In fact, oligonucleotides with CpG motifs were shown to stimulate IL-6 and IL-12 production by monocytes [15]. So far, ten TLRs have been identified in mammalian systems [23,24]. TLRs are broadly expressed in various tissues and the complete panel of TLR mRNA is expressed in the spleen and peripheral blood [25,26]. The greatest variety of TLR mRNAs is found in specialized phagocytes, suggesting a key role for TLRs in innate immunity. Endotoxin, a compound that is known to cause skin inflammation, is recognized by TLR4. In general, the recognition of ligands by TLRs causes stimulation and activation of signaling pathways that end in NF-kB activation, resulting in the induction of many immunomodulating molecules.

In this study, we intradermally injected plasmid DNA into ear skin, and noted an approximately 40% decrease in the ear swelling in TLR9-knockout mice compared with TRL9 (+/+) littermates. This inhibition suggested that plasmid-DNA-induced dermatitis was mediated mostly by TLR9. However, a decrease of 40% implies that pathways other than TLR9 might be involved in the reaction. In this study, we were aware that even small amounts of endotoxin contamination can worsen the skin plasmid DNA reaction. Although endotoxin and plasmid DNA basically interact with different TLRs, TLR4 and TLR9, respectively, both stimulate the same signaling pathway resulting in NF-kB activation. Therefore, increases in endotoxin levels can additively or synergistically worsen the skin reaction caused by plasmid DNA. We therefore insist on the strict avoidance of any endotoxin contamination in the clinical use of the naked plasmid DNA injection technique, especially

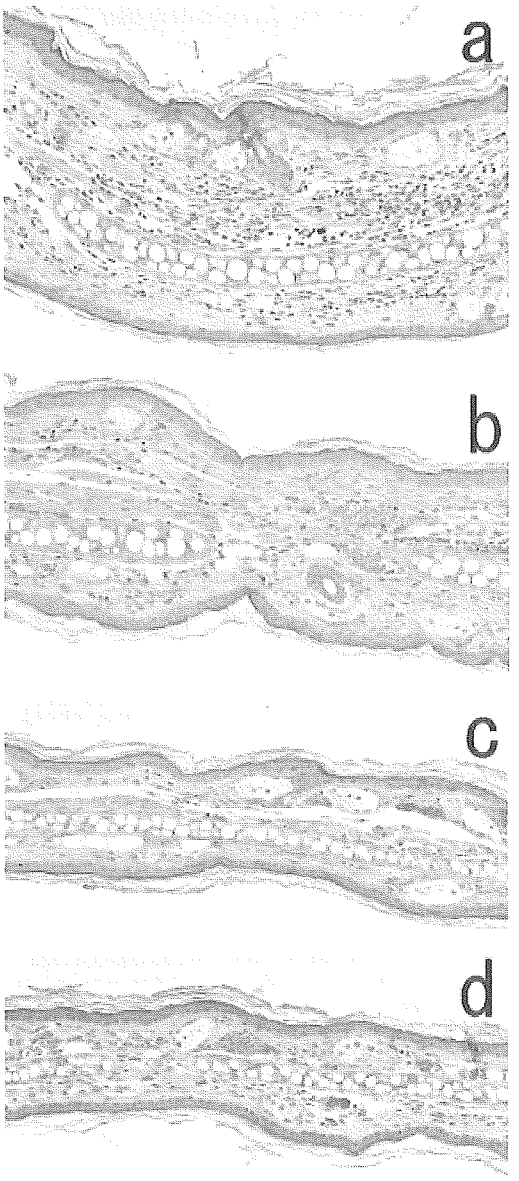

Figure 7. Histological demonstration of a decrease in the plasmid-DNA-induced inflammation reaction in TLR9-knockout mice. We injected the Gel-treated BS and Calf DNA into the right ears of TLR9-knockout mice (TLR9 −/−) and wild-type littermates (TLR9 +/+), and the treated ears were examined histologically 48 h after the injection. (a) TLR9+/+ with plasmid, (b) TLR9 −/− with plasmid, (c) TLR9 +/+ with Calf DNA, and (d) TLR9 −/− with Calf DNA

in the skin. We recommend that clinical-grade plasmids should be used for even experimental animals in similar future experiments. Furthermore, since the reaction was dose-dependent on the amount of plasmid DNA, it seems important that we should determine the precise minimal dose of DNA for the most efficient expression in human keratinocytes.

Acknowledgements

The authors wish to thank James R. McMillan for his critical reading of and comments on this manuscript. This work

was supported in part by Grants-in-Aid from the Ministry of Education, Science, Sports, and Culture of Japan (15390337 to DS, 13357008 to HS and 15390336 to HS) and by grants from the Ministry of Health of Japan (H13- Specific Disease-02 to HS).

References

1. Edelstein ML, Abedi MR, Wixon J, *et al.* Gene therapy clinical trials worldwide 1989–2004 – an overview. *J Gene Med* 2004; **6**: 597–602.
2. Vogel JC. Keratinocyte gene therapy. *Arch Dermatol* 1993; **129**: 1478–1483.
3. Khavari PA. Gene therapy for genetic skin disease. *J Invest Dermatol* 1998; **110**: 462–467.
4. Meng X, Sawamura D, Tamai K, *et al.* Keratinocyte gene therapy for systemic diseases: circulating interleukin-10 released from gene-transferred keratinocytes inhibits contact hypersensitivity at distant areas of the skin. *J Clin Invest* 1998; **101**: 1462–1467.
5. Ghazizadeh S, Taichman LB. Virus-mediated gene transfer for cutaneous gene therapy. *Hum Gene Ther* 2000; **11**: 2247–2251.
6. Vogel JC. Nonviral skin gene therapy. *Hum Gene Ther* 2000; **11**: 2253–2259.
7. Hengge UR, Chan EF, Foster RA, *et al.* Cytokine gene expression in epidermis with biological effects following injection of naked DNA. *Nature Genet* 1995; **10**: 161–166.
8. Hengge UR, Walker PS, Vogel JC. Expression of naked DNA in human, pig, and mouse skin. *J Clin Invest* 1996; **97**: 2911–2916.
9. Sawamura D, Ina S, Itai K, *et al.* In vivo gene introduction into keratinocytes using jet injection. *Gene Ther* 1999; **6**: 1785–1987.
10. Sato M, Sawamura D, Ina S, *et al.* In vivo introduction of the interleukin-6 (IL-6) gene into human keratinocytes: introduction of epidermal proliferation by the fully spliced form of IL-6, but not by the alternative spliced form. *Arch Dermatol Res* 1999; **291**: 400–404.
11. Baumgartner I, Pieczek A, Manor O, *et al.* Constitutive expression of phVEGF165 after intramuscular gene transfer promotes collateral vessel development in patients with critical limb ischemia. *Circulation* 1998; **97**: 1114–1123.
12. Vale PR, Losordo DW, Milliken CE, *et al.* Left ventricular electromechanical mapping to assess efficacy of phVEGF(165) gene transfer for therapeutic angiogenesis in chronic myocardial ischemia. *Circulation* 200; **102**: 965–974.
13. Sawamura D, Meng X, Ina S, *et al.* In vivo transfer of a foreign gene to keratinocytes using the hemagglutinating virus of Japan-liposome method. *J Invest Dermatol* 1997; **108**: 195–199.
14. Guthrie LA, McPhail LC, Henson PM, *et al.* Priming of neutrophils for enhanced release of oxygen metabolites by bacterial lipopolysaccharide. *J Exp Med* 1984; **160**: 1656–1671.
15. Hemmi H, Takeuchi O, Kawai T, *et al.* A Toll-like receptor recognizes bacterial DNA. *Nature* 2000; **408**: 740–745.
16. Schwartz DA, Quinn TJ, Thorne PS, *et al.* CpG motifs in bacterial DNA cause inflammation in the lower respiratory tract. *J Clin Invest* 1997; **100**: 68–73.
17. Deng GM, Nilsson IM, Verdrengh M, *et al.* Intra-articularly localized bacterial DNA containing CpG motifs induces arthritis. *Nat Med* 1999; **5**: 702–705.
18. Ishikawa Y, Kirikae T, Hirata M, *et al.* Local skin response in mice induced by a single intradermal injection of bacterial lipopolysaccharide and lipid A. *Infect Immunol* 1991; **59**: 1954–1960.
19. Glasspool-Malone J, Somiari S, Drabick JJ, *et al.* Efficient nonviral cutaneous transfection. *Mol Ther* 2000; **2**: 140–146.
20. Dujardin N, Van Der Smissen P, Preat V. Topical gene transfer into rat skin using electroporation. *Pharm Res* 2001; **18**: 61–66.
21. Krieg AM. Direct immunologic activities of CpG DNA and implications for gene therapy. *J Gene Med* 1999; **1**: 56–63.
22. Yamamoto S, Yamamoto T, Tokunaga T. Oligodeoxyribonucleotides with 5′-ACGT-3′ or 5′-TCGA-3′ sequence induce production of interferons. *Curr Top Microbiol Immunol* 2000; **247**: 23–39.
23. Takeda K, Kaisho T, Akira S. Toll-like receptors. *Annu Rev Immunol* 2003; **21**: 335–376.
24. Underhill DM. Toll-like receptors: networking for success. *Eur J Immunol* 2003; **33**: 1767–1775.
25. Zarember KA, Godowski PJ. Tissue expression of human Toll-like receptors and differential regulation of Toll-like receptor mRNAs in leukocytes in response to microbes, their products, and cytokines. *J Immunol* 2002; **168**: 554–561.
26. O'Neill LA. Immunology. After the toll rush. *Science* 2004; **303**: 1481–1482.

Gene Therapy (2005) 12, 857–861

www.nature.com/gt

BRIEF COMMUNICATION

Beta defensin-3 engineered epidermis shows highly protective effect for bacterial infection

D Sawamura[1], M Goto[1], A Shibaki[1], M Akiyama[1], JR McMillan[1], Y Abiko[2] and H Shimizu[1]
[1]Department of Dermatology, Hokkaido University Graduate School of Medicine, Sapporo; and [2]Department of Oral Pathology, Health Sciences University of Hokkaido, Ishikari-Tobetsu, Japan

Defensins are small cationic proteins that harbor broad-spectrum microbicidal activity against bacteria, fungi and viruses. This study examines the effects on pathogens of the epidermis engineered to express human beta-defensin 3 (HBD3) to combat bacterial infections. First, we examined the localization of HBD3 in the epidermis and observed HBD3 in the intercellular spaces and lamellar bodies of the upper epidermal layers. This result showed HBD3 expressed and assembled in the outer layers of the epidermis was suspected to counter the invading microorganisms. Next, we established a keratinocyte cell line that stably expressed HBD3 and found that the culture medium showed antibacterial activity. Furthermore, we prepared an epidermal sheet of these cells with the HBD3 gene and grafted this onto a dermal wound on a nude rat. The HBD3 engineered epidermis demonstrated significant antimicrobial activity. Skin ulcers without epidermis are constantly exposed to invading microorganisms. Biopsy samples of re-epithelizing epidermis from patients with skin ulcers were collected, and HBD3 mRNA level measured in the epidermis. The epidermal samples from the ulcer skin expressed 2.5 times higher levels of HBD3 transcript than those in the control skin. These results, taken together, indicate that the therapeutic introduction of the HBD3 gene into somatic cells may provide a new gene therapy strategy for intractable infectious diseases.
Gene Therapy (2005) **12,** 857–861. doi:10.1038/sj.gt.3302472; Published online 24 February 2005

Keywords: *keratinocyte; skin; infectious disease; psoriasis*

The skin is always exposed to invading microorganisms, and is accordingly armed with several efficient defence systems. The synthesis of small, antimicrobial peptides was discovered within the last decade and these peptides are highly effective in directly killing microorganisms. The small (3–5 kDa) cationic defensins represent a critical peptide group among a growing number of microbicidal peptides that are capable of a broad spectrum of antimicrobial activity against many Gram-negative and Gram-positive bacteria, fungi, and certain viruses.[1,2]

Mammal defensins comprise genetically distinct α- and β-subfamilies of cationic tri-disulfide bridges. In humans, four types of human β-defensins (HBD), HBD1 through to 4 have been characterized thus far.[3–6] HBD1, 2 and 3 have been identified in human skin and keratinocytes. HBD1 was initially isolated from hemofiltrates[3] and found to be constitutively expressed in various epithelia.[7] However, HBD1 does not appear as abundantly in the epidermis and is not upregulated in response to inflammation as are the other defensins.[5] HBD2 was isolated from the skin of patients with psoriasis and its expression was found in epithelial cells of the skin and the lung. HBD2 is inducible upon treatment with proinflammatory cytokines including TNF-α and interleukin 1, and when in contact with *Pseudomonas aeruginosa* bacteria.[8] HBD3 has also been isolated from psoriatic skin.[5] HBD1 and HBD2 shows antimicrobial activity predominantly against Gram-negative bacteria and these peptides are inactivated in physiologic salt concentrations, while HBD3 has a salt-insensitive broad spectrum activity that kills both Gram-negative and -positive bacteria including *P. aeruginosa*, *Streptococcus pyogenes*, multiresistant *Staphylococcus aureus*, and vancomycin-resistant *Enterococcus faecium*.

The use of conventional antibiotics provides the most powerful means to treat bacterial infections. However, the development of bacterial resistance against conventional antibiotics has emerged as a major public health concern. The appearance of resistant bacteria has been directly linked to the misuse and overuse of antibiotics in humans as well as in farm animals. This situation calls for the development of alternative strategies and therapies to fight infection. Defensins may turn out to be antibacterial agents with low susceptibility to resistance mechanisms, and thus gene therapy using these or the related genes is of great potential for treating intractable infectious diseases.[9–11]

As mentioned above, HBD3 is salt-insensitive and is effective for Gram-positive bacteria, which are common cause of the skin infection. In this study, we introduced the HBD3 gene into a keratinocyte cell line and prepared the epidermal graft overexpressing HBD3 to determine the usefulness or feasibility of HBD3 engineered epidermis as a novel antibacterial therapy.

Correspondence: Professor D Sawamura, Department of Dermatology, Hokkaido University Graduate School of Medicine, N15 W7, Sapporo 060-8638, Japan
Received 4 August 2004; accepted 22 December 2004; published online 24 February 2005

We first examined the localization of HBD3 in normal human control skin. Immunohistochemical analysis demonstrated that HBD3 was located predominantly in the upper spinous and granular layers of the epidermis (Figure 1a). Immunoelectron microscopy showed gold particles in the intercellular spaces of the stratum corneum (Figure 1b). Additionally, gold staining was observed in intracellular membrane-bound vacuoles, close to the apical surface of the granular layer plasma membrane presumed to be lamellar bodies (Figure 1c). Also we used cathepsin D antibodies as control, because cathepsin D is a well-known component localized within lamellar bodes.[12,13] Immunoelectron microscopy of similar sections (Figure 1d) stained with both these antibodies showed that cathepsin D was also expressed within the lamellar body-like membrane-bound vacuoles just beneath the apical granular layer plasma membrane similar to HBD3.

Recently, HBD2 has also been shown to localize to the lamellar bodies and keratinocyte intercellular spaces.[14] Lamellar bodies used to be thought of as discrete granules that transport the contents from the Golgi apparatus to intercellular space. Recent evidence, however, has suggested a membrane folding model, in which the trans-Golgi network, lamellar bodes and intercellular space are all part of the same continuous membrane structure.[13,15] In this system, the synthesized molecules are easily released into the extracellular space through a cell surface pore via a continuous membrane-bound tube. Since the lamellar body was first found exclusively associated with the outer surface of the stratum granulosum, a lamellar body-related secretory system must be present to enable high concentration of HBD2 and HBD3 molecules to reach the outer layer of the epidermis and form a defensive barrier containing enough HBD2 and 3 to be effective.

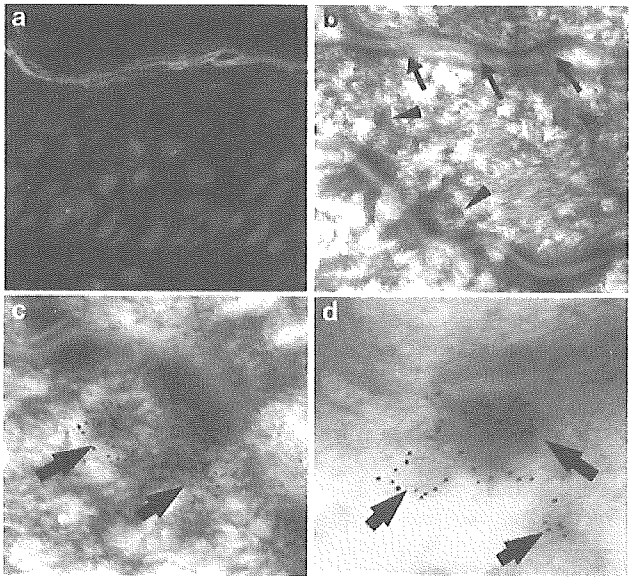

Figure 1 *(a) The localization of HBD3 was examined. Skin cryosections were cut from the biopsy skin specimens taken from normal volunteers and were incubated with the anti-human HBD3 rabbit polyclonal antibody (Novus Biologicals, Littleton, CO, USA). The second antibodies were goat anti-rabbit immunoglobulins conjugated to fluorescein (FITC). Immunostaining was detected as green (FITC) and the nuclear stain was observed as red (propidium iodide). HBD3 was located predominantly in the spinous and granular layers of the epidermis. (b–d) Immunoelectron microscopic analysis was performed. Normal skin samples were cryofixed with liquid propane cooled nitrogen, cryosubstituted at −80°C and low temperature embedded at −60°C in Lowicryl K11 M resin undergoing UV polymerization. Ultrathin sections were cut and immunogold stained using a 5 nm gold conjugated secondary (British Biocell, Cardiff, UK).[17] The anti-human HBD3 antibody and the anti-human cathepsin D rabbit polyclonal antibody (Santa Cruz Biotechnology, Santa Cruz, CA, USA) were used as primary antibodies and then a goat anti-rabbit IgG gold-conjugated secondary antibody (British Biocell, Cardiff, UK) was used. Gold particles were observed in the intercellular spaces of the stratum corneum (→) and in lamellar bodies of intracellular spaces (▼) often seen immediately beneath the apical plasma membrane of granular layer keratinocytes. Magnification: HDB3; (b) 25 000 ×, (c) 60 000 ×; cathepsin D; (d) 60 0000 ×.*

To establish a keratinocyte cell line that stably expresses HBD3, we first introduced the plasmid pFRT/lacZeo (Invitrogen, Carlsbad, CA, USA) into a human keratinocyte cell line, HaCaT cells, and subsequently prepared the Flp-In-HaCaT cells with the integrated Flp recombination target (FRT) site, which were also stably expressing β-galactosidase from the plasmid. Then, HBD3 cDNA was integrated into the FRT site already in the Flp-In-HaCaT cell genome, resulting in the establishment of an HBD3-HaCaT cell line. Immunostaining using anti-HBD3 antibodies showed that the cultured HBD3-HaCaT cell line expressed significant amounts of HBD3 (data not shown).

Our ultrastructural study showed that HBD3 was normally secreted though a special secretory system closely related to or identical with lamellar bodies *in vivo* (Figure 1). We then wondered whether this transgene synthesis and transfer from keratinocytes was released HBD3 into the culture medium. Before examining the culture medium, the activity of synthetic HBD3 was estimated using Gram-positive *S. aureus* strains ATCC6538 (AT), SA015 (SA-1) and SA092 (SA-2). Synthetic HBD3 showed almost the same antimicrobial activity against the three *S. aureus* strains (Figure 2a). It started to show killing activity in the microgram order and the concentration necessary to kill 50 % bacteria of SA-1 was approximately 8 μg/ml. Subsequently, colony-forming assays were performed to determine the antibacterial activity of HBD3-HaCaT cell culture medium. The apparent antimicrobial activity found from the 25 × concentrated sample and 50% killing activity was observed in the 100 × concentrated sample in SA-1 (Figure 2b). The supernatant of Fip-in-HaCaT cells as a control exhibited no killing activity against the bacteria. To determine the precise concentration of HBD3 in the culture medium, we performed immunodot blot analysis. The concentration of HBD3 in HBD3-HaCaT cell culture medium was 9.2 ng/ml (Figure 3c), while those of HaCaT and the Flp-In-HaCaT cells showed little or no detectable amount. Comparison with the result of synthetic HBD3 (Figure 2a) suggested that recombinant HBD3 from HaCaT cells had more antimicrobial activity than synthetic HBD3.

An epidermal sheet of HBD3-HaCaT cells was prepared and grafted onto an artificially induced ulcer in a nude rat (Figure 3a (1–3)). Immunohistochemical analysis using an anti-HBD3 antibody found strong reactivity in the graft, HBD3 engineered epidermis, while little or no reactivity was seen in the control epidermis of grafted Flp-In-HaCaT cells (Figure 3a (4,5)). The expression of HBD3 was stronger in the upper layers than the lower layers of the epidermis. On the other hand,

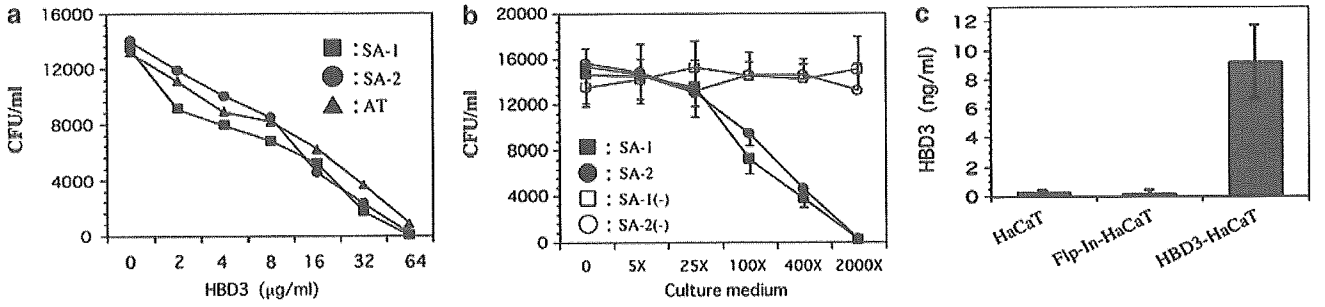

Figure 2 *(a) Peptide HBD3 was chemically synthesized according to the cDNA sequence.[5] Bacterial strains, Gram-positive S. aureus: ATCC6538 (AT), SA015 (SA-1) and SA092 (SA-2), used for experiments. SA-1 and SA-2 were isolated from patients with skin infection that was sensitive to antibiotics and kindly given by Fujisawa Pharmaceutical Co., Ltd, Osaka, Japan. The bacteria were incubated with synthetic HBD3 in 200 μl of 10 mM sodium phosphate buffer (pH 7.4) containing 1% trypticase soy broth for 3 h at 37°C. We measured the antimicrobial activity of HBD3 using the same media as used in the previous paper.[5] The antibiotic activity was estimated by plating serial dilutions of the incubation mixture and calculation of the colony-forming unit (CFU) after 24 h. (b) The human keratinocyte cell line HaCaT[18] was maintained in Dulbecco's modified Eagles's medium with 10% fetal bovine serum. Flp-In system (Invitrogen, Carlsbad, CA, USA) was utilized for generating stable expression cell line. In this system, Flp recombinase-mediated recombination occurs between specific Flp Recombination Target (FRT) sites. To integrate the FRT site into the genome of HaCaT cells, we first introduced plasmid pFRT/lacZeo and selected for Flp-In-HaCaT cells by medium containing zeocin. Fip-in-HaCaT cells expressed a lacZ-Zeocin fusion gene could be also detected by β-galactosidase staining. To amplify the coding regions of HBD3 cDNA by PCR, we synthesized two primer sets, 5′-TTTAAGCTTAGCAGCTATGAG GATCC-3′ and 5′-GGGCTCGAGGGTTTTTATTTCTTTC-3′ for the HBD3 cDNA. PCR was performed with oligo-(dT)-primed human keratinocyte cDNA as template. The PCR fragments were digested with restriction enzymes and subcloned into a multicloning site of plasmid pcDNA5/FRT, in which the inserted cDNA was driven by the CMV promoter. We performed co-transfection of the pcDNA5/FRT with HBD3 cDNA and the Flp recombinase expression vector pOG44. Finally, Flp-In-HaCaT cells with integration of HBD3 cDNA were selected by medium containing hygromycin. The cell line was referred as HBD3-HaCaT cell. The culture medium without antibiotics and fetal calf serum collected, treated with Centricon YM-3 Centrifugal Filter Unit (Millipore: Bedford, MA, USA) for concentration and desalting and subjected to colony-forming assay. Each value shown represents the mean±s.d. of three individual samples. (● ■) HBD3-HaCaT cell, (○ □) Flp-In-HaCaT as control. (c) The concentration of HBD3 in the culture medium was determined by immunodot blot analysis.[16] Positive control and standard curve were generated with synthetic HBD3 peptides. Briefly, 5 μl of the concentrated medium (from the above samples) and serially diluted synthetic HBD3 were dotted in triplicate on nitrocellulose membrane. The membrane was incubated with the anti-human HBD3 rabbit polyclonal antibodies at 4°C overnight, and then reacted with goat anti-rabbit antibodies conjugated with peroxidase at room temperature for 2 h. The resultant dot complexes were processed for Phototope HRP Western Blot Detection System (Cell Signaling, Beverly, MA, USA) according to the manufacturer's protocol. The amount shown represents the mean±s.d. of three individual samples.*

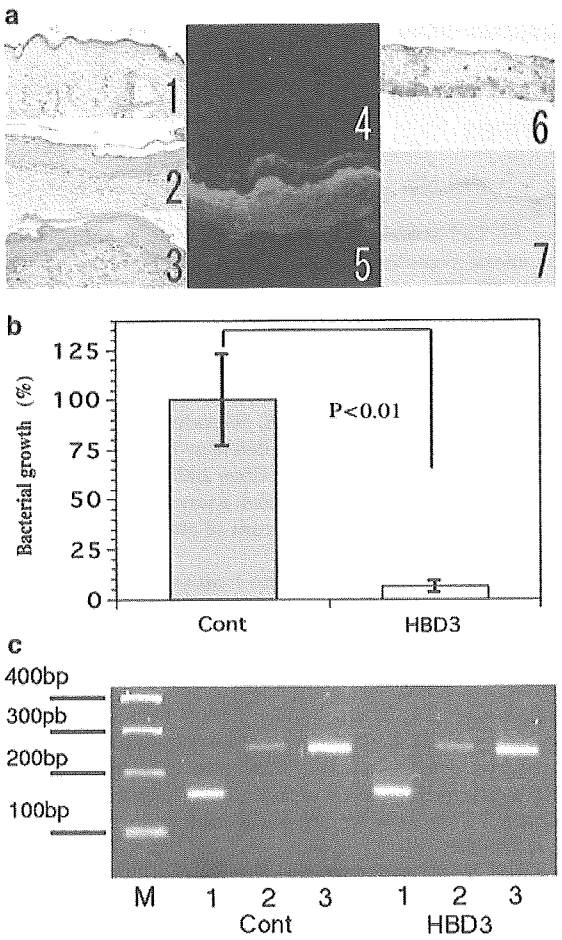

Figure 3 *(a) In nude rats (F344/N Jcl-rnu), the sites for transplantation were prepared by excising a 2 cm² area of dorsal epidermis and dermis. The confluent cultures of HBD3-HaCaT and control Flp-In-HaCaT were treated with dispase (1 nU/ml:Godo Shusei, Japan), and the floating epidermal sheet was placed on the prepared site of the nude rat. An occlusive dressing was quickly placed over the graft to hold it in position and to prevent it from drying. After 7 days, the skin sample was taken by excision. Afterwards, routine hematoxylin-eosin staining (1–3), immunostaining of the HBD3 antibody (4,5) and β-galactosidase staining (6,7) were performed. (1) normal rat; (2,4,6) the skin from Flp-In-HaCaT; (3,5,7) the skin from HBD3-HaCaT. (b) At 5 days after transplantation, the serial dilution of bacterial culture of SA-1 was applied to the graft and was overlaid with an occlusive dressing in wet condition. After 8 h incubation, the samples were collected from the surface of the graft with a sterile cotton swab, and transferred to the culture medium. The CFU was measured by plating. In each experiment, the CFU from the sample of HBD3-HaCaT was expressed as the rate against that of control Flp-In-HaCaT. Each group consisted of five rats and each value shown represents the mean±s.d. of five individual samples. The student t-test detected a significant difference, $P<0.01$; Cont versus HBD3. (c) We excised the rat epidermis surrounding both the control and HBD3 grafts. Epidermal sheets were obtained from the skin samples by treatment with 10 mg/ml dispase (3 h at 37°C).[19] Keratinocyte suspensions were obtained from these epidermal sheets by a further 0.25% trypsin treatment (30 min at 37°C). Total RNA was extracted from cultured cells and first strand cDNA was synthesized with reverse transcriptase (Life Sciences Inc., St Petersburg, FL, USA) using an oligo-dT primer. PCR was performed using following primers: 5′-GACACCAATCTCTACCGTCT-3′ and 5′-ACCGGAAAGG CTGTATACCA-3′ for rat CRAMP (GenBank accession no. AF484553); 5′-ATTTCTCCTGGTGCTGCTGT-3′ and 5′-CTTGCAGCATCTCACTC TAG-3′ for rat BD3 (NM 022544); 5′-AGCTGAACGGGAAGCTCACT-3′ and 5′-CATTGAGAGCAATGCCAGCC-3′ for rat GAPDH (NM 017008) as control. (M) 100 bp size marker, (1) BD3 (147 bp), (2) CRAMP (250 bp), (3) GAPDH: (246 bp).*

β-galactosidase staining showed strong activity in the control epidermis, but not in the HBD3 engineered epidermis (Figure 3a (6,7)). To ascertain the precise antimicrobial activity of the engineered skin, we applied bacteria SA-1 to the grafted epidermis and performed a colony-forming assay. The results demonstrated that significant antibacterial activity ($P<0.01$) was present in the HBD3 engineered epidermis compared with the control epidermis (Figure 3b). We examined the effect of the rat's endogenously produced antimicrobial peptides from the surrounding skin of the HBD3 and control grafts, but could not detect difference in expression of rat cathelicidine cathelin-related antimicrobial peptide (CRAMP) or BD3 (Figure 3c).

We demonstrated HBD3 killing activity in the culture medium; however, the HBD3 concentration in the supernatant was only 9.2 ng/ml, which was insufficient for significant antimicrobial activity. Therefore, we postulated that this HBD3 engineered epidermis might not show any significant antibacterial activity *in vivo*. However, our results showed that the HBD3 gene transfected epidermis formed an effective barrier that could withstand the attack of invading bacteria. These data suggested that the conditions *in vivo* might be a more suitable environment for keratinocytes to produce HBD3 and also utilize a more 'normal' lamellar body-related secretory system already in place for HBD3 in the appropriate position to prevent or protect from micro-organism attack.

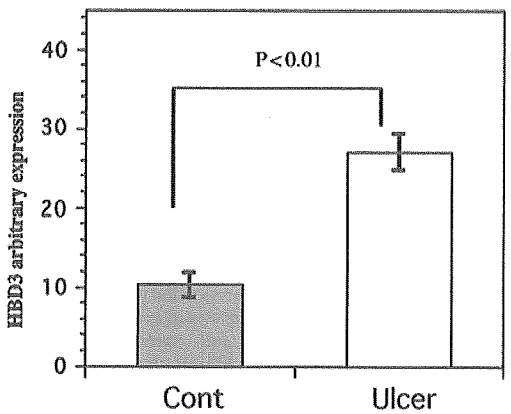

Figure 4 *The skin samples were collected from six patients with skin ulcer resulting from trauma and deep dermal burn during treatment at the Hokkaido University Hospital. Informed consent was obtained from individual subjects. We selected the patients with re-epithelizing ulcers at the healing stage, but the ulcer was so large that complete epithelization was expected to take a considerable time and to lead to hypertrophic scar formation. During operations we removed the skin samples from the ulcer with 0.5 cm margin. To prepare keratinocytes, we first separated the epidermis from dermis and subcutaneous tissue. Normal skin samples were obtained from seven patients undergoing reconstructive plastic surgery. Epidermal sheets were obtained from the skin samples by treatment with 10 mg/ml dispase (3 h at 37°C).[19] Keratinocyte suspensions were obtained from these epidermal sheets by a further 0.25% trypsin treatment (30 min at 37°C). Total RNA was extracted from cultured cells and first strand cDNA was synthesized with reverse transcriptase (Life Sciences Inc., St Petersburg, FL, USA) using an oligo-dT primer. Assays-on-Demand™ Products for HBD3 and GAPDH were purchased from Applied Biosystems (Foster City, CA, USA). The 50 μl reaction in each well contained 1 μl of total cDNA, 300 nm of sequence-specific primers and 200 nm of dual-labeled fluorogenic probe in 1 Taqman Universal PCR master mix (Applied Biosystems). A negative PCR control without template and a positive PCR control with a template of known amplification were included in each assay. The reaction was performed in an ABI PRISM 7700 Sequence Detection System. The HBD3 specific signal was normalized by constitutively expressed GAPDH and expressed as arbitrary scale. Ulcer: ulcer skin samples, Cont: normal skin samples. Each value indicated the mean±s.d. The student's t-test detected a significant difference, $P<0.01$; Cont versus Ulcer.*

One of the worst situations for preventing the tissue from bacterial invasion is in skin ulcers without any epidermal covering. If HBD3 plays a critical role in defending bacterial invasion in the skin, we hypothesized that re-epithelizing epidermis surrounding the ulcer wound might express a much higher level of HBD3. We therefore collected skin samples from patients with skin ulcers and examined the expression of HBD3 mRNA levels in the epidermis. As we expected, the epidermal samples in the ulcer skin expressed 2.5 times higher levels of HBD3 transcript than those in control skin (Figure 4). This result also suggested an increase in defensin expression as one of the major antimicrobial defense systems that can form an effective response to protect tissue from bacterial invasion.

Atopic dermatitis is a chronic inflammatory intractable skin disorder with unknown etiology. Atopic dermatitis skin lesions are often associated with higher than normal bacterial and viral infections, and atopic dermatitis skin has demonstrated a significant decrease expression of cathelicidin LL-37 and HBD2.[16] This evidence also led us to introduce the HBD3 gene into the epidermis and we have proved that the HBD3 gene transfected epidermis had a highly protective shield against bacterial invasion. The gene therapeutic introduction of HBD3 gene or the related genes into somatic cells may provide a new strategy for gene therapy for intractable infectious diseases.

References

1 Ganz T, Selsted ME, Lehrer RI. Defensins. *Eur J Haematol* 1990; **44**: 1–8.
2 Lehrer RI, Lichtenstein AK, Ganz T. Defensins: antimicrobial and cytotoxic peptides of mammalian cells. *Annu Rev Immunol* 1993; **11**: 105–128.
3 Bensch KW *et al*. hBD-1: a novel beta-defensin from human plasma. *FEBS Lett* 1995; **368**: 331–335.
4 Harder J, Bartels J, Christophers E, Schroder JM. A peptide antibiotic from human skin. *Nature* 1997; **387**: 861.
5 Harder J, Bartels J, Christophers E, Schroder JM. Isolation and characterization of human beta-defensin-3, a novel human inducible peptide antibiotic. *J Biol Chem* 2001; **276**: 5707–5713.
6 Garcia JR *et al*. Human beta-defensin 4: a novel inducible peptide with a specific salt-sensitive spectrum of antimicrobial activity. *FASEB J* 2001; **15**: 1819–1821.
7 Valore EV *et al*. Human beta-defensin-1: an antimicrobial peptide of urogenital tissues. *J Clin Invest* 1998; **101**: 1633–1642.
8 Harder J *et al*. Mucoid *Pseudomonas aeruginosa*, TNF-alpha, and IL-1beta, but not IL-6, induce human beta-defensin-2 in respiratory epithelia. *Am J Respir Cell Mol Biol* 2000; **22**: 714–721.
9 Bals R, Weiner DJ, Meegalla RL, Wilson JM. Transfer of a cathelicidin peptide antibiotic gene restores bacterial killing in a cystic fibrosis xenograft model. *J Clin Invest* 1999; **103**: 1113–1117.
10 Nikol S *et al*. Needle injection catheter delivery of the gene for an antibacterial agent inhibits neointimal formation. *Gene Therapy* 1999; **6**: 737–748.
11 Huang GT *et al*. A model for antimicrobial gene therapy: demonstration of human beta-defensin 2 antimicrobial activities *in vivo*. *Hum Gene Ther* 2002; **13**: 2017–2025.

12 Horikoshi T *et al.* Role of endogeneous cathepsin D-like and chymotrypsin-like proteolysis in human epidermal desquamation. *Br J Dermatol* 1999; **141**: 453–459.
13 Ishida-Yamamoto A *et al.* Epidermal lamellar granules transport different cargoes as distinct aggregates. *J Invest Dermatol* 2004; **122**: 1137–1144.
14 Oren A, Ganz T, Liu L, Meerloo T. In human epidermis, beta-defensin 2 is packaged in lamellar bodies. *Exp Mol Pathol* 2003; **74**: 180–182.
15 Norlen L. Skin barrier structure and function: the single gel phase model. *J Invest Dermatol* 2001; **117**: 830–836.
16 Fellermann K, Wehkamp J, Stange EF. Antimicrobial peptides in the skin. *N Engl J Med* 2003; **348**: 361–363.
17 Simizu H, McDonald JN, Kennedy AR, Eady RA. Demonstration of intra- and extracellular localization of bullous pemphigoid antigen using cryofixation and freeze substitution for embedding immunoelectron microscopy. *Arch Dermatol Res* 1989; **106**: 443–448.
18 Boukamp P *et al.* Normal keratinization in a spontaneously immortalized aneuploid human keratinocyte cell line. *J Cell Biol* 1988; **106**: 761–771.
19 Sawamura D *et al.* Induction of keratinocyte proliferation and lymphocytic infiltration by *in vivo* introduction of the IL-6 gene into keratinocytes and possibility of keratinocyte gene therapy for inflammatory skin diseases using IL-6 mutant genes. *J Immunol* 1998; **161**: 5633–5639.

J Hum Genet (2005) 50: 543–546
DOI 10.1007/s10038-005-0290-4

SHORT COMMUNICATION

**Daisuke Sawamura · Maki Goto · Kana Yasukawa
Kazuko Sato-Matsumura · Hideki Nakamura · Kei Ito
Hiroyuki Nakamura · Yuki Tomita · Hiroshi Shimizu**

Genetic studies of 20 Japanese families of dystrophic epidermolysis bullosa

Received: 30 June 2005 / Accepted: 27 July 2005 / Published online: 28 September 2005

Abstract Dystrophic EB (DEB) is clinically characterized by mucocutaneous blistering in response to minor trauma, followed by scarring and nail dystrophy, and is caused by mutations in the *COL7A1* gene encoding type VII collagen. DEB is inherited in either an autosomal dominant (DDEB) or recessive (RDEB) fashion. DDEB basically results from a glycine substitution mutation within the collagenous domain on one *COL7A1* allele, while a combination of mutations such as premature stop codon, missense, and splice-site mutations on both alleles causes RDEB. In this study, mutation analysis was performed in 20 distinct Japanese DEB families (16 RDEB and four DDEB). The result demonstrated 30 pathogenic *COL7A1* mutations with 16 novel mutations, which included four missense, five nonsense, one deletion, two insertion, one indel, and three splice-site mutations. We confirmed that Japanese *COL7A1* mutations were basically family specific, although three mutations, 5818delC, 6573 + 1G > C, and E2857X, were recurrent based on previous reports. Furthermore, the Q2827X mutation found in two unrelated families would be regarded as a candidate recurrent Japanese *COL7A1* mutation. The study furthers our understanding of both the clinical and allelic heterogeneity displayed in Japanese DEB patients.

Keywords Type VII collagen · Mutation · COL7A1 · Blister · Glycine substitution

D. Sawamura (✉) · M. Goto · K. Yasukawa
K. Sato-Matsumura · H. Nakamura · K. Ito · H. Nakamura
Y. Tomita · H. Shimizu
Department of Dermatology, Hokkaido University Graduate School of Medicine, North 15 West 7, Kita-ku, Sapporo 060-8638, Japan
E-mail: smartdai@med.hokudai.ac.jp
Tel.: +81-11-7067387
Fax: +81-11-7067820

Introduction

Epidermolysis bullosa (EB) comprises a group of cutaneous hereditary mechanobullous disorders that can be classified into three major categories, the simplex, the junctional, and the dystrophic forms, on the basis of the level of tissue separation within the basement membrane zone (BMZ; Fine et al. 2000). Dystrophic EB (DEB) is clinically characterized by mucocutaneous blistering in response to minor trauma, followed by scarring and nail dystrophy, in which patients exhibit tissue separation beneath the lamina densa at the level of the anchoring fibrils. It occurs as either an autosomal dominant (DDEB) or recessive (RDEB) trait, each form having a different specific clinical presentation and severity (Fine et al. 2000).

Both DDEB and RDEB are caused by mutations in the *COL7A1* gene encoding type VII collagen, the major component of anchoring fibrils (Uitto et al. 1995; Fine et al. 2000). The most severe RDEB subtype, the Hallopeau–Siemens (HS) type, shows a complete lack of expression of type VII collagen, whereas some collagen expression is found in the non-Hallopeau–Siemens (nHS) type. Clinical features of DDEB are comparatively milder than those of RDEB. To date, several hundred pathogenic mutations within the collagenous and noncollagenous domains of type VII collagen gene have been identified in different forms of DEB (Christiano et al. 1995; Uitto et al. 1995; Shimizu et al. 1996; Pulkkinen and Uitto 1999; Whittock et al. 1999). Although particular molecular and phenotypic characteristics of DEB have been elucidated, we cannot always expect DEB clinical manifestations precisely from genetic information of *COL7A1*. Furthermore, no systematic study has thus far revealed detailed delineation of *COL7A1* mutations in Japanese DEB patients apart from several recurrent *COL7A1* mutations (Tamai et al. 1999; Murata et al. 2004).

In this study, we performed mutational analysis of 20 Japanese DEB families and have demonstrated the

characteristic features of *COL7A1* mutations in Japanese DEB patients.

Materials and methods

Subjects

Twenty unrelated Japanese DEB families, who had been referred to Hokkaido University Hospital's special clinic for inherited skin disorders from January 2000 to December 2004, were studied (Table 1). DEB was at first clinically diagnosed and later confirmed by immunofluorescence antigen mapping that demonstrated tissue separation beneath the lamina densa. Clinical features and inheritance modes also helped to differentiate most, though not all, cases into recessive or dominant DEB subtypes. Immunofluorescence expression of type VII collagen was of significant diagnostic value in determining HS-RDEB and nHS-RDEB.

Immunohistochemical analysis

Skin biopsies were taken from DEB patients and subjected to a routine immunofluorescence antigen mapping study (Shimizu et al. 1996). The specimens were embedded in OCT compound, and 10-μm thick sections were cut. The following monoclonal antibodies (mAbs) against BMZ components were used: mAbs HD1-121 for plectin; GoH3 and 3E1 (Chemicon International, CA, USA) for the α6 and β4 integrins, respectively; GB3 (Sera-lab, Cambridge, UK) for laminin 5; LH7.2 (Sigma, St. Louis, MO, USA) for type VII collagen; and S1193 and HDD20 for BPAG1 and BPA2, respectively. The antibodies GoH3, S1193, and HDD 20 were kind gifts from Dr. A. Sonnenberg of the Netherlands Cancer Institute. The antibody HD1-121 was also a kind gift from Dr. K. Owaribe of Nogoya University. The bound antibodies were detected with FITC-conjugated goat anti-mouse IgG antibody. In some cases, nuclei were counterstained with propidium iodide.

All DEB patients in this study were evaluated by several experienced dermatologists. This study was approved by the Ethical Committee at Hokkaido University Graduate School of Medicine. Informed consent was obtained from individual patients or their parents.

Mutation analysis

Genomic DNA was isolated from peripheral lymphocytes of patients and their families using standard procedures. *COL7A1* segments including all 118 exons, all exon-intron borders, and the promoter region were amplified by PCR using pairs of oligonucleotide primers synthesized on the basis of intronic sequences according to the report by Christiano et al. (1997; GenBank numbers L02870 and L23982). The PCR products were examined on 2% agarose gel and subjected to direct automated nucleotide sequencing using the BigDye

Table 1 Clinical phenotype, type VII collagen expression, and *COL7A1* mutations in patients in this study

Family	Age/sex (proband)	Phenotype	VII expression	Mutation	Effect
1	1 year/F	nHS-RDEB	+	R1340X/C2875F	PTC/Mis
2	44 years/F[a]	nHS-RDEB	+	G1815R/5818delC	GS/PTC
3	40 years/M	nHS-RDEB	+	E2857X/5604 + 2G > C	PTC/SS
4	7 years/M[a]	nHS-RDEB	+	G1595R/Q2827X	GS/PTC
5	1 year/F	nHS-RDEB	+	8109 + 2T > A/6573 + 1G > C	SS/SS
6	9 years/M	nHS-RDEB	+	8358 + 1G > T/G2366C	SS/GS
7	5 years/M	nHS-RDEB	+	R1957Q/6573 + 1G > C	Mis/SS
8	37 years/M	nHS-RDEB	+	Q2827X/ND	PTC/ND
9	7 days/F	nHS-RDEB	+	R236X/ND	PTC/ND
10	32 years/F	nHS-RDEB	+	R1978X/ND	PTC/ND
11	2 months/M[b]	HS-RDEB	−	434insGCAT/R2261X	PTC/PTC
12	1 week/M	HS-RDEB	−	R137X/Q641X	PTC/PTC
13	1 year/M	HS-RDEB	−	1474del8/5818delC	PTC/PTC
14	3 days/M	HS-RDEB	−	R1683X/6081insC	PTC/PTC
15	3 years/F	HS-RDEB	−	5818delC/ND	PTC/ND
16	7 years/M	HS-RDEB	−	ND/ND	ND/ND
17	1 month/F	DDEB	+[c]	G2037E	GS
18	4 years/F	DDEB	+	G2064E	GS
19	23 years/M	DDEB	+	G2034R	GS
20	26 years/M	DDEB	+	8069del17insGA	GS

Novel mutations are underlined

RDEB recessive dystrophic epidermolysis bullosa; *DDEB* dominant dystrophic epidermolysis bullosa; *HS* Hallopeau-Siemens; *nHS* non-Hallopeau-Siemens; *GS* glycine substitution mutation; *PTC* premature stop codon mutation; *Mis* missense mutation; *SS* splice-site mutation; *ND* not detected

[a] Families 2 and 4 with unusual clinical phenotype were published in a case report (Sato-Matsumura et al. 2002; Tomita et al. 2003)

[b] Family 11 was also published (Sato-Matsumura et al. 2003)

[c] Retention of type VII collagen in keratinocytes

Terminator System (Applied Biosystems, Foster City, CA, USA).

Results and discussion

An increasing number of DEB mutations have elucidated some general genotype-phenotype correlations (Jarvikallio et al. 1997; Pulkkinen et al. 1999). DDEB patients basically harbor glycine substitution mutations within the collagenous domain on one *COL7A1* allele, leading to disruptions in anchoring fibril assembly and relatively mild clinical features. On the other hand, patients with RDEB in its most severe form, the Hallopeau–Siemens variant (HS-RDEB), frequently have premature termination codon (PTC) mutations on both alleles. These mutations characteristically lead to nonsense-mediated mRNA decay that manifests as a complete absence of type VII collagen protein and total loss of anchoring fibrils. On the other hand, patients with the non-Hallopeau–Siemens variant (nHS-RDEB) show milder phenotype, and type VII collagen can be generally detected immunohistologically. This DEB subtype is caused by a combination of mutations such as PTC, missense, and splice-site mutations on both alleles.

The routine immunofluorescence antigen mapping study in a blister site showed that all BMZ antigens were located in the roof of the blister, indicating tissue separation beneath the lamina densa. Also, linear type VII collagen expression was found along the dermal epidermal junction in nHS-RDEB and DDEB patients, whereas HS-RDEB cases showed no expression (Table 1). We found retention of type VII collagen within epidermal keratinocytes in a DDEB (family 17, data not shown).

Examination of 40 alleles of 20 families (10 nHS-RDEB, six HS-RDEB, and four DDEB) identified 30 pathogenic *COL7A1* mutations, including 16 novel mutations (Table 1). *COL7A1* mutations of nHS-RDEB included five missense mutations [G1595R(4783G > A), G1815R(5443G > A), R1957Q(5870G > A), G2366C (7096G > T), C2875F(8627G > T)], five nonsense mutations [R236X(706C > T), R1340X(4018C > T), R1978X (5932C > T), Q2827X(8479C > T), E2857X(8569G > T)], one insertion-deletion mutation (5818delC), and four splice-site mutations (5604 + 2G > C, 6573 + 1G > C, 8109 + 2T > A, 8358 + 1G > T). HS-RDEB patients showed four nonsense mutations [R137X(409C > T), Q641X(1921C > T), R1683X(5047C > T), R2261X (6781C > T)] and four insertion-deletion mutations (434insGCAT, 1474del8, 5818delC, 6081insC). As predicted by previous DEB mutation reports, all combinations of PTC mutations caused HS-RDEB, while nHS-RDEB resulted from compound heterozygous *COL7A1* mutations except for homozygous nonsense PTC/PTC mutations. Although we could not find positional effect of PTC mutations as suggested by the previous report (Tamai et al. 1999), final conclusions need further accumulation of RDEB patients with PTC mutations.

In DDEB patients, we identified three dominant glycine substitution mutations [G2034R (6100G > A), G2037E (6110G > A), G2064E (6191G > A)]. These glycine substitution mutations were previously reported, and, interestingly, the nucleotide changes were identical to those in previous reports (Kon et al. 1997; Rouan et al. 1998; Jonkman et al. 1999; Whittock et al. 1999; Lee et al. 2000). Glycine residues within the collagenous domain are critical for proper triple helix formation. Some *COL7A1* glycine substitution mutations, which cause RDEB in association with a second mutation on the other allele, are silent in patients with a normal COL7A1 allele. In addition, heterozygous glycine substitution mutations can cause DDEB through dominant negative interference of the collagen triple helix. Although this study also identified both dominant and recessive glycine substitution mutations (Table 1), we could not clarify positional effect of glycine substitution on the inheritance mode. A single indel mutation, 8069del17insGA, was novel. The 17-nucleotide deletion from 8069 to 8084 with GA insertion resulted in a 15-nucleotide deletion within the collagenous domain, which failed to change an open reading frame of *COL7A1* but interfered with the collagen triple helix (Gly-X-Y). This mutation causes a DDEB phenotype, probably in a dominant negative fashion.

We failed to detect one allelic mutation in families 8, 9, 10, and 15, and both allelic mutations in RDEB family 16 (Table 1). Thus, this study could demonstrate *COL7A1* mutations in 30 out of 36 alleles that were expected to have *COL7A1* mutations, and the resulting ratio of successful mutation detection was 83%. Similar, large-scale *COL7A1* mutation reports using Italian patient data also failed to determine single allele mutations in 13 RDEB families out of a total of 49 families (Gardella et al. 2002). This suggests at least two possibilities: that pathogenic mutations lie in the other parts of the *COL7A1* gene that were not examined in these studies, and that genes other than *COL7A1* are responsible for the DEB phenotype.

Although *COL7A1* mutations are generally family specific, some recurrent mutations have been reported in several populations: R2814X, R578R, and 7786delG in British patients (Mellerio et al. 1997); 2470insG in Mexican patients (Salas-Alanis et al. 2000); and 8441-14del21, 4783-1G > A, 497insA, and G1664A in Italian patients (Gardella et al. 2002). In Japanese patients, the mutations 5818delC (nine out of 50 cases: 18%), 6573 + 1G > C (6/50:12%), and E2857X (9/50:18%) are present only in individuals of Japanese ethnic origin (Tamai et al. 1999). The present study also detected 5818delC in four families, 6573 + 1G > C in two families, and E2857X in one family out of total of 20 unrelated families. Furthermore, the Q2827X mutation was found in two unrelated families, and this mutation should be regarded as a candidate recurrent Japanese COL7A1 mutation. However, 16 mutations were novel out of a total of 30 pathogenic DEB mutations identified, indicating that Japanese *COL7A1* mutations are family